

REVIEW ARTICLE

Smart implants: 4D-printed shape-morphing scaffolds for medical implantation

Guiwen Qu^{1†}, Jinjian Huang^{1†}, Guosheng Gu¹, Zongan Li^{2*}, Xiuwen Wu^{1*}, Jianan Ren^{1*}

¹Research Institute of General Surgery, Jinling Hospital, School of Medicine, Southeast University, Nanjing 210009, China

²Jiangsu Key Laboratory of 3D Printing Equipment and Manufacturing, NARI School of Electrical and Automation Engineering, Nanjing Normal University, Nanjing 210042, China

Abstract

Biomedical implants have recently shown excellent application potential in tissue repair and replacement. Applying three-dimensional (3D) printing to implant scaffold fabrication can help to address individual needs more precisely. Four-dimensional (4D) printing emerges rapidly based on the development of shape-responsive materials and design methods, which makes the production of dynamic functional implants possible. Smart implants can be pre-designed to respond to endogenous or exogenous stimuli and perform seamless integration with regular/irregular tissue defects, defect-luminal organs, or curved structures via programmed shape morphing. At the same time, they offer great advantages in minimally invasive surgery due to the small-to-large volume transition. In addition, 4D-printed cellular scaffolds can generate extracellular matrix (ECM)-mimetic structures that interact with the contacting cells, expanding the possible sources of tissue/organ grafts and substitutes. This review summarizes the typical technologies and materials of 4D-printed scaffolds, and the programming designs and applications of these scaffolds are further highlighted. Finally, we propose the prospects and outlook of 4D-printed shape-morphing implants.

Keywords: 4D printing; Shape-morphing scaffolds; Medical implants; Tissue engineering; Minimally invasive surgery

[†]These authors contributed equally to this work.

***Corresponding authors:**

Zongan Li
(zongan_li@njnu.edu.cn)

Xiuwen Wu
(wuxiuwen@njnu.edu.cn)

Jianan Ren
(jiananr@njnu.edu.cn)

Citation: Qu G, Huang J, Gu G, et al., 2023, Smart implants: 4D-printed shape-morphing scaffolds for medical implantation. *Int J Bioprint*, 9(5): 764. <https://doi.org/10.18063/ijb.764>

Received: February 17, 2023

Accepted: April 18, 2023

Published Online: May 30, 2023

Copyright: © 2023 Author(s).

This is an Open Access article distributed under the terms of the Creative Commons Attribution License, permitting distribution, and reproduction in any medium, provided the original work is properly cited.

Publisher's Note: Whioce Publishing remains neutral with regard to jurisdictional claims in published maps and institutional affiliations.

1. Introduction

Nowadays, as the gap between growing demands for personalized medical care and shortage of available treatments widens, biomedical implants, which are able to repair and replace tissues in regenerative medicine, start to show huge potential as a treatment. They are utilized to renovate, support, replicate, or ameliorate the functions of native tissues or organs^[1]. With the development of biomaterial researches, a variety of implants with therapeutic or regenerative functions are applied in human body to enhance the quality of patient lives, such as bone implants^[2], vascular implants^[3], and so forth. Their future demand is also expected to increase^[4].

Three-dimensional (3D) printing, widely known as additive manufacturing, provides technical support for effectively generating medical implants with complex morphology or fulfilling individual requirements^[1]. It has been widely applied in healthcare due to its advantage in developing manufacturing methods for many specific products. It simplifies production processes, saves time, reduces costs, and promotes the innovation of medical models^[5]. The remarkable applications of 3D printing in tissue engineering with the aid of clinical imaging information are the generation of scaffolds for the repair and replacement of body defects or diseased parts^[6,7].

Most biological tissues present more complicated forms and possess unique functions through dynamic changes^[8], posing a new challenge to medical implants. Meanwhile, the widespread use of minimally invasive surgery also has placed demands on implants. The static structures produced by 3D printing may not satisfy the growing expectation of implants. Under this request, four-dimensional (4D) printing has emerged at the right moment, along with the diversity of materials and the development of processing methods, incorporating the fourth dimension, "time." In detail, it has the capacity to present conformational changes under one or more specific stimuli such as temperature, pH, light, water, and others^[9]. It overcomes the weaknesses of 3D printing that only considers the initial status of printed objects and is limited to creating static products^[10,11]. Based on this superiority of bionic capacity, it has great application prospects to fabricate dynamic scaffolds to satisfy specific demands of implantation sites or approaches. Specifically, 4D-printed scaffolds show great advantages in adapting to the dynamic structure of human organs and tissues^[12,13] and applying to minimally invasive surgery. More interestingly, they have ability to respond to specific external or physiological conditions^[6] (solvent, temperature, pH, etc.) by design to realize time-dependent physical changes or replicate the dynamic biological behavior of native tissues for better adaptation to the body environment. Thus, they play a role in repairing tissue defects intelligently. Furthermore, 4D dynamic supports are more beneficial for cell attachment and subsequent orientation, proliferation, and differentiation^[14]. On this account, biomimetic cellular scaffolds can be made for tissue repair and functional tissue substitutes.

Several challenges present during the manufacturing process of 4D dynamic medical implants: (i) selection of stimuli-responsive materials that possess printability, biocompatibility, and biodegradability; (ii) application of printing technologies; (iii) design of deformation strategies; (iv) aimed at specific application scenarios. Therefore, this review systematically reports typical technologies and

materials of 4D-printed scaffolds. Then programming designs and applications of these scaffolds are highlighted. Finally, we propose the prospects and outlook of 4D-printed shape-morphing scaffolds (Figure 1).

2. 4D printing technologies

Three-dimensional (3D) printing is a general technology that manufactures 3D objects layer by layer by steadily adding materials or inks in accordance with the imported pre-defined digital models^[15]. 4D printing is based on its core technology, considered as an extension of 3D printing. The printing processes are mainly extrusion-based printing (fused deposition modeling (FDM), direct ink writing (DIW)), and light-assisted printing (digital light processing (DLP), stereolithography (SLA), selective laser sintering (SLS), selective laser melting (SLM), and inkjet printing)^[16]. An overview of various technologies is given in this section.

One of the most often used techniques is extrusion-based printing, which prints objects along pre-determined horizontal and vertical pathways as materials flow through print nozzles. FDM melts solid filaments by heating the nozzle to the melting temperature of materials and then squeezes the materials out on the platform along the planned path. Thermoplastic materials, including polyurethane (PU), polylactic acid (PLA), polyamide (PA), and acrylonitrile butadiene styrene (ABS), are generally used in FDM to fabricate thermo-responsive biological implants with good mechanical properties^[1]. Running FDM is cheap and easy to operate; however, the printing resolution is relatively low. On the other hand, DIW extrudes ink through its nozzle to build complex geometric objects layer by layer. It works mainly for liquid inks with shear-thinning behavior, thermosetting, or light-curing property, which is also friendly to cell-laden bioinks. It can print one or more materials simultaneously and has been in extensive use to build bionic heterogeneous and gradient structures, such as human skin^[17] and musculoskeletal scaffolds^[18].

The light-assisted printing is another widely used printing process, where a laser beam or a UV light performs as a light source to initiate photocuring to solidify photocrosslinkable liquid polymer or resin layer by layer to form a structure (the former is called SLA, and the latter is called DLP)^[19]. It is also popular in the fabrication of bioscaffolds for tissue engineering, and its improved resolution makes the formation of subtle and complex structures possible^[20]. SLS/SLM sinters powdered materials under laser, and a new layer is laid after one layer is cured, so the process is repeated to obtain specific structures. Common materials used in SLS/SLM include polymers

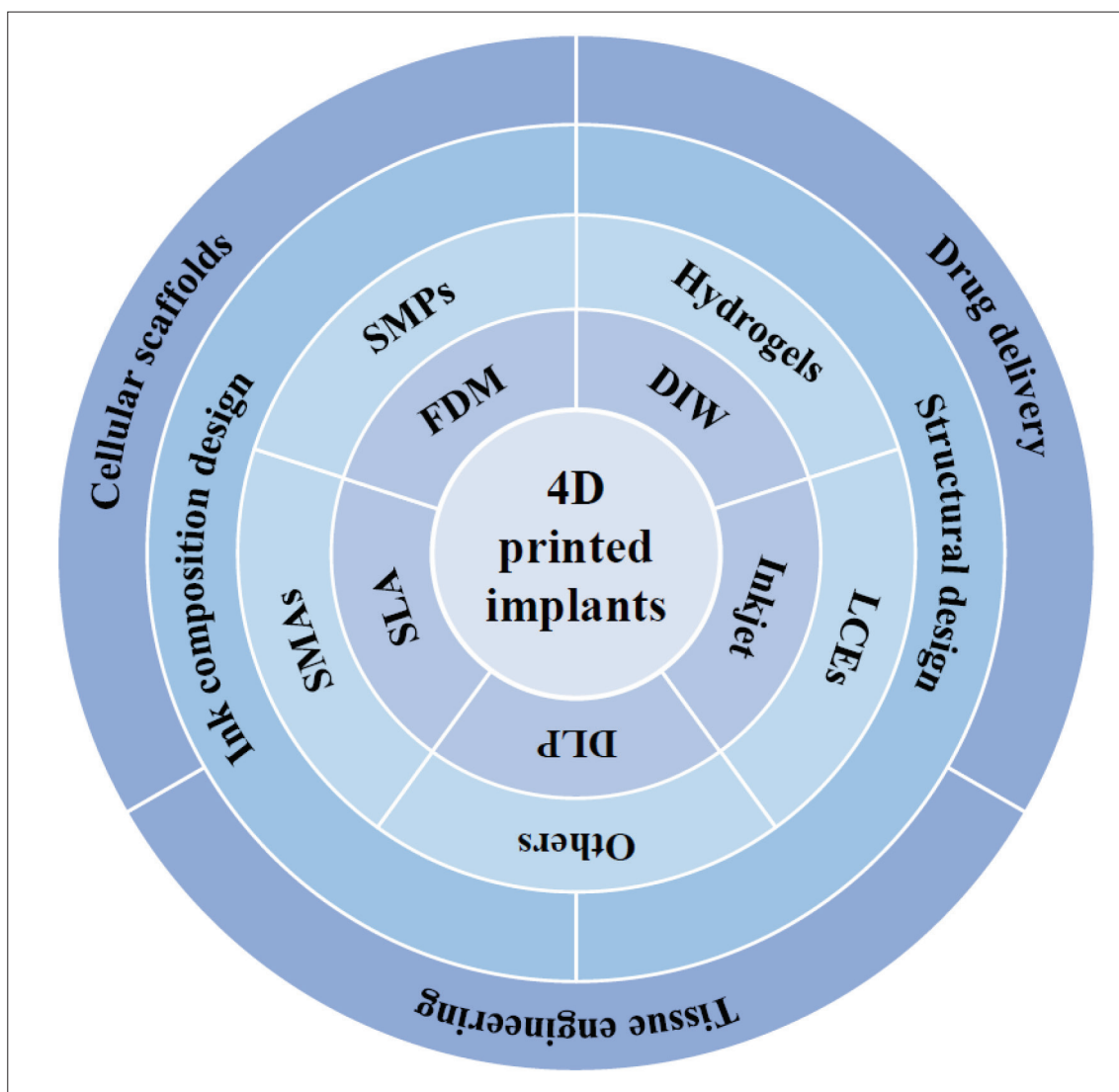


Figure 1. Challenges in the manufacturing process of 4D-printed medical implants and the main contents of this review.

such as PU and PA, metals, and ceramic powders. Shape memory ceramics and alloy materials commonly reported in 4D printing can be processed with this technology^[21]. Inkjet printing is a non-contact printing technique that generates droplet inkjets onto the substrate under pressure and solidifies layer by layer through UV light^[15,19,22]. It is capable of printing objects with high fidelity due to its high resolution of 50–500 μm ^[1,20], and printing bioink with cell clusters is made possible with this special printing method.

3. Materials

The success of the fabrication of 4D-printed implants mainly depends on the utilization of shape-responsive materials (SRMs). The common SRMs often contain shape memory polymers (SMPs), stimuli-responsive hydrogels,

shape memory alloys (SMAs), liquid crystal elastomers (LCEs), and their composites^[22,23].

3.1. Shape memory polymers (SMPs)

Shape memory polymers (SMPs) provide a great shape memory effect (SME). They can be activated by external stimuli and restored to their original shape subsequently^[24,25]. Their shape change includes two states: temporary programmed shape and permanent recovery shape. For example, thermo-responsive SMPs contain two keypoints at the molecular level; one is a “switch” that has a thermal transition at transition temperature values (T_g) and forms physical crosslinks to fix at the temporary shape; the other is a “net-point” that determines the permanent shape. Macroscopically, the shape of SMPs can be programmed under external

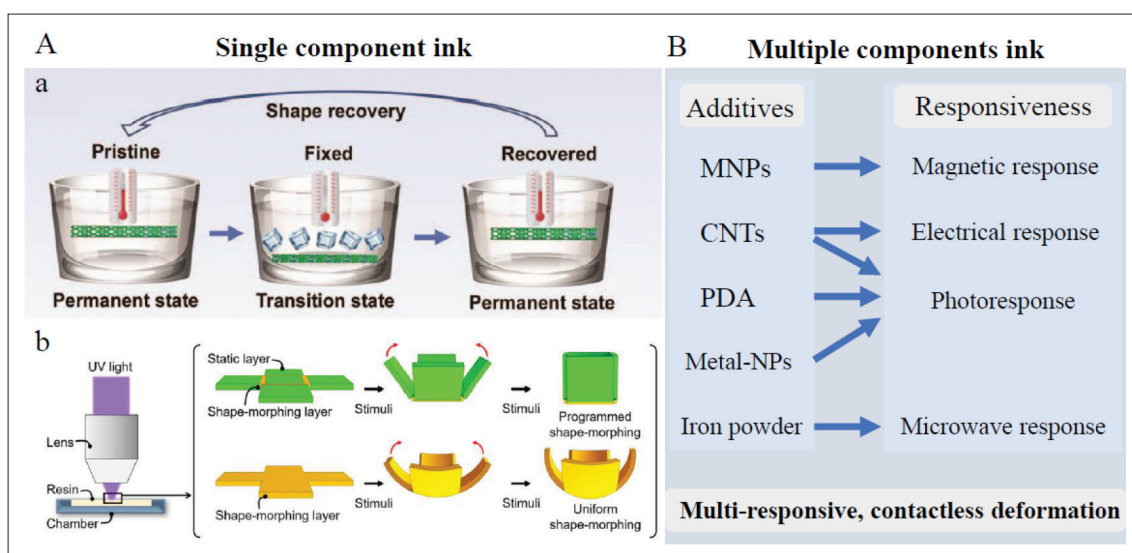


Figure 2. Design of printing ink in 4D structures. (A) 4D scaffolds made by single-component ink printing, a) self-deploying process of the peripheral vascular stent based on PLA^[60]. Copyright 2022, Royal Society of Chemistry. b) Deforming process by simple pattern design via a mask film in a single layer of PNIPAM hydrogel^[61]. Copyright 2022, MDPI. (B) Adding different materials into a poly network to realize multiple and complex responsive behaviors. CNTs: carbon nanotubes; metal-NPs: metal-nanoparticles; MNPs: magnetic nanoparticles; PDA: polydopamine; PLA: polylactic acid; PNIPAM: poly (N-isopropylacrylamide).

stress when the ambient temperature is above T_g and keeps stable at a cooled temperature. Once the temperature increases above T_g , the shape recovers. Correspondingly, shape transformation is the result of molecular chain conformation changing at the molecular level^[26]. This process is reversible and can be easily predicted and repeated by accurate measurement of the pre-programming scheme^[27]. Direct thermal activation of SMPs to initiate macroscopic deformation is the most common method in 4D programming. Due to their flexible shape memory effects, good biodegradability, and good biocompatibility, SMPs have been widely applied in the fabrication of bioscaffolds^[28-31]. SMPs commonly used in the fabrication of smart implants include PU, polycaprolactone (PCL), PLA, and recently discovered soybean oil epoxidized acrylate (SOEA)^[32-34]. Medical implants prepared from SMPs can be temporarily fixed in a contracted or folded state to facilitate passage through minimally invasive surgical wounds. Its shape restores to its initial shape after being placed in the specific site. During this process, the mechanical damage to the wound is greatly reduced. By identifying the shape of defects in specific sites in advance, setting as the initial shape of printed SMPs, then pre-programming so as to implant, the shape can be restored after implantation to repair defects seamlessly, which is more conducive to the subsequent renovation of tissues^[35]. Furthermore, many kinds of fillers can be incorporated into the SMP matrix to form shape memory polymer composites (SMPCs)^[26,36,37] to optimize responsive temperature, responsive

deformation modes, and mechanical behavior of SMP-based scaffolds in order to better cater to body desire. For example, some structures introduce active substances into SMPs polymer networks (such as carbon nanotubes (CNTs)^[38], magnetic nanoparticles (MNPs)^[39], etc.) to realize 4D dynamic functionalities under various non-contact stimuli, and this will be described at length in the later section.

3.2. Stimuli-responsive hydrogels

Hydrogels, defined as hydrophilic polymeric materials, are attractive for biomedical implants for their similarity to biological tissues in structures and characteristics^[23,40]. In general, they form insoluble networks by inner covalent or physical crosslinking of hydrophilic polymers^[41]. The stimuli-responsive ability of hydrogels depends on their volume changes caused by water absorption or desorption that are influenced by pH, temperature, ion concentration, and some biomedical signals^[23,42,43]. Combined with 4D printing, they are endowed with more application potential in tissue reconstruction, drug delivery, etc. Among them, poly (N-isopropylacrylamide) (PNIPAM) is a typical thermo-sensitive hydrogel for its lower critical solution temperature (LCST) at $\sim 32^\circ\text{C}$, which is close to human body temperature^[44]. It is hydrophobic when placed in an environment with a temperature above its LCST; on the contrary, it becomes hydrophilic^[45]. This phenomenon appears as its volume variation with temperature. However, weak mechanical strength limits the use of hydrogels. Secondary polymeric

networks are introduced to combat this limitation in the fabrication of smart scaffolds^[22]. For instance, interpenetrating network hydrogels consisting of ionic and covalently bonded crosslinked polymer networks are designed to increase application potential^[46]. Besides, many strategies have been proposed to design hydrogel-based deforming scaffolds on the basis of their natural properties, and we will make a detailed elaboration in the following section.

3.3. Shape memory alloys (SMAs)

Shape memory alloys (SMAs) are materials with the shape memory effect that transforms thermal energy into mechanical energy^[47]. They can return to their original shapes even after strong deformation, which attributes to their phase change under the external stimulus. This superelastic behavior as well as their satisfactory biocompatibility and corrosion resistance make SMAs an ideal choice for biomedical uses^[48,49]. Particularly, nickel-titanium (NiTi) alloy performs best in shape recovery and superelastic strain, resulting in extensive application in clinic orthopedics^[47,50]. However, the restricted flexibility of alloy materials, which leads to compliance mismatch, limits their application in implantation for soft tissue engineering.

3.4. Liquid crystal elastomers (LCEs)

Liquid crystal elastomers (LCEs) are polymer networks with anisotropic liquid crystalline properties while maintaining the properties of elastomers^[51]. They are another representative intelligent material that shows large and reversible shape changes under external stimuli (heat, light, electricity, magnetism, pH, solvent, etc.)^[23]. They shift phase state or molecular structure that causes a change in the arrangement order of liquid crystal elements when heated above their nematic-to-isotropic transition temperature (T_{NI}). The removal of external stimuli causes LCEs to return to their original shape reversibly. This process reflects the deformation of materials macroscopically. Huge advances have been achieved in LCEs for medical application recently^[52-54]. They have shown a great promising application in artificial muscles^[55], actuators, and sensors due to their excellent driving performance, mechanical properties, and biocompatibility^[56].

3.5. Other materials

Apart from the above materials that react to external stimuli directly, a variety of other active, inactive, or multi-component materials have also displayed their dynamic deformability that conduces to the generation of 4D constructs. For example, certain ceramics possess high energy output and high-temperature usage, and can serve as a possible class of smart materials^[57-59]. More relevant materials contributing to the generation of 4D

implants through particular programming designs will be elaborated on in the next section.

4. Deformation design

The 4D deformation of biomedical implants presents as self-rolling, self-bending, self-expanding, and self-folding. Designs of printed ink composition and structures allow the implementation of various complex deformations under different physical, chemical, or physiological stimulation. These, in turn, facilitate a wide range of applications of 4D-printed implants for different organizational structures under different physiological conditions. In this section, we will expound on mechanisms of dynamic deformations from the aspects of ink composition design and structural design. These design methods can unite with each other to create complex multi-responsive structures.

4.1. Design of ink composition

The ink components play an important role in the design of 4D structures. Constructs composed of single or multiple materials can both demonstrate shape transformation due to different mechanisms, and we will detail the two aspects.

4.1.1. Single-component ink

Single-component ink printing (SMPs, hydrogels, SMAs, LCEs, etc.) can achieve the expected 4D deformation effect through a simple program. The shape change mainly depends on the temperature-response property of the materials applied. For example, 4D-printed peripheral vascular stents based on PLA via an FDM printer were proposed in Wang's study, and its shape memory effect was based on the transition between the glassy state and rubbery state of SMPs (Figure 2Aa)^[60]. The findings show that 4D implants can be prepared as required using single-shape memory material.

Apart from the simple single-material printing, some ingenious pattern designs have been introduced into single-component printing based on the former. For example, a single-layer 4D-printed object based on individual PNIPAM hydrogel was obtained by different UV-focusing times of static and shape-morphing parts with the help of a mask film. This led to different coefficients of thermal expansion in different parts and subsequent thermal-induced deformation (Figure 2Ab)^[61]. Through the printing of single-component ink and surface pattern design, 4D scaffolds can be generated quite simply, and the subsequent shape-morphing process can be actuated immediately.

4.1.2. Multiple components ink

The responsive modes of single-material-based 4D printing are usually simplistic. Some other substances are added into polymer networks to realize multiple and complex

responsive behaviors. Adding MNPs into the printing ink is one of the methods to fabricate 4D constructs that can be actuated by external magnetic fields. Magnetite ferroferric oxide (Fe_3O_4) microparticles are the most commonly used^[39,62-64]. In this way, contactless control of product deformation under a magnetic field can be realized. By combining SMPs with MNPs, the composite simultaneously presents thermo- and magnetic-responsive shape-morphing behavior^[39]. Printed implants possess electroactive shape memory performance by adding CNTs into printing ink^[65,66], and implants that incorporate SMPs with CNTs have dual stimulus responsiveness similarly.

Some studies embedded particular substances in the printed SMP/SMA-based shape memory composites to convert other forms of energy into thermal energy and thus deform the structure. Materials like the CNTs mentioned earlier, polydopamine (PDA), and some metal nanoparticles are provided with photothermal conversion properties. Some studies reported shape memory frameworks with near-infrared light (NIR) or other light responsiveness by the addition of CNTs^[67], PDA^[68,69], gold nanoparticles^[70], or copper sulfide nanoparticles (CuSNPs)^[71] in the precursor ink. In addition, Koh *et al.* presented ferromagnetic PLA actuated by microwave radiation. The iron powder functioned as heater elements and triggered non-contact and localized deformation by placing strategically^[72].

We discovered that multiple materials printing could potentially acquire leapfrogging from contact to contactless deformation controlling, from single to multiple stimulus response, that extends their application prospects (Figure 2B). Non-contact stimulus response is also necessary for the design of smart implants. *In vivo* deformation can be realized under *in vitro* stimulation by remote contactless control to trigger the subsequent deformation process, which broadens application scenarios of 4D implants. At the same time, the biocompatibility of composite structures should also be taken into account.

4.2. Design of printed structures

Various smart designs in structures represent significant breakthroughs for 4D printing methods. Numerous design schemes have sprung up recently. Proceeding from the basic properties of materials, these designs recreate dynamic biomimetic processes and functions. We will make an integrated discussion from three aspects: (i) bi-/multi-layer structure design; (ii) gradient structure design; (iii) origami structure design.

4.2.1. Bi-/multi-layer structure design

The manufacture of bi-/multi-layer structures is a popular design in 4D printing, which has been demonstrated effective in dynamic structure building. These constructs

have two basic components: a driving layer and a passive layer. The anisotropy of swelling or shrinkage behaviors between these layers is a basic driving mechanism.

As hydrophilic polymer networks, the crosslinking density and solvent type can affect the swelling property of hydrogels. The swelling difference between hydrogel layers in a solvent can lead the entirety of construction to self-bend^[73-75]. For instance, bilayer hydrogels based on different concentrations of silk fibroin bioink were prepared, and shape bending was obtained due to anisotropic volume change of different layers in an aqueous solution. Moreover, a reversible de-bending process was discovered in saltwater because of the trigger of osmotic action by salt. This reversible deformation process is precisely dependent on the volume change induced by water absorption and dehydration behavior of the driving layer in different osmotic pressure solutions (Figure 3Aa)^[76]. Beyond this, some materials show pH-dependent swelling behavior as a result of the electrostatic repulsion of the charged unit at the molecular level. On this basis, pH-sensitive bilayer structures whose geometric changes were actuated by imbalanced swelling behavior under different pH conditions can be fabricated (Figure 3Ab)^[77]. Some hydrogels, such as sodium alginate, show ion responsiveness and exhibit 4D deformation in ionic solution by design^[78]. More impressively, stimuli-responsive material in a recent study was generated and actuated by volume change in the driving layer, which integrated genetically engineered yeast that only proliferated with the presence of particular biomolecules. This method provided for the production of bioactive scaffolds and devices responsive to biological stimulation^[79].

The volume change differences under particular conditions also exist in elastomers and other materials. The high swellable driving layer can be designed by embedding low boiling point microliquid chambers^[80,81] or thermally expanding microspheres (TEM)^[82] in elastomers. In the former, liquid-vapor-phase change of microliquid chambers such as ethanol when heated or cooled causes volume change of the driving layer and thus actuates bilayer structures to curve reversibly (Figure 3Ac). The process is reversible. Moreover, extra filling of thermally conductive material particles such as liquid metal fillers provides faster thermal response speed^[80,81]. In contrast, the deformation caused by the thermal expansion coefficient with a large difference in two layers due to the existence of TEMs in the latter is irreversible^[82]. Another study innovatively presented a bilayer structure (one layer of elastomer and another layer of transition material) actuated by combined stimuli of heat and ethanol. The structure was programmed to curve in 60°C ethanol because the elastomer swelled via ethanol diffusion,

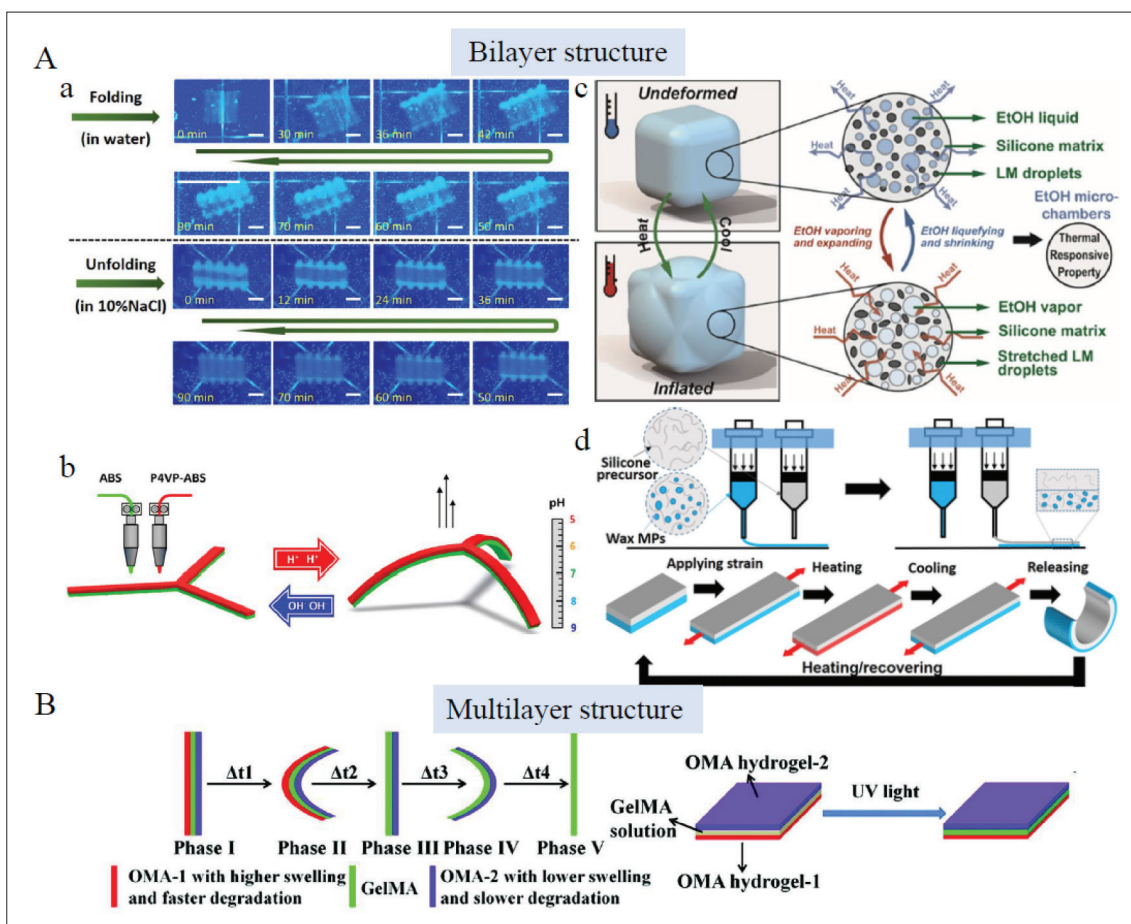


Figure 3. Bi-/multi-layer structure design in 4D printing. (A) Bilayer structural design, a) Reversible transformation of bilayer hydrogel induced by water absorption and dehydration behavior of driving layer in different osmotic pressure solutions^[76]. Copyright 2020, Elsevier. b) A pH-sensitive claw deforming caused by anisotropic volume change in an aqueous solution under different pH conditions^[77]. Copyright 2022, Elsevier. c) Volume change of the driving layer caused by liquid–vapor-phase change of ethanol micro chambers when heated or cooled^[81]. Copyright 2020, American Chemical Society. d) 4D deforming procedures powered by a pre-stored stress field in the driving layer consisting of wax microparticles^[84]. Copyright 2021, American Chemical Society. (B) Multi-layer structural design, a trilayer structure consisting of two outer oxidized methacrylated alginate (OMA) layers with different swelling and degradation capacities and a GelMA layer underwent five phases of deformation due to anisotropic swelling of the three layers and the degradation of the fast-degradation layer^[89]. Copyright 2021, Wiley-VCH. LM: Liquid metal; MP: Microparticle; OMA: Oxidized and methacrylate alginate.

and the transition material reduced its stiffness to reshape easily. Dry heating at 70°C boosted ethanol evaporation, and the shape recovered^[83]. In these conditions, various 4D design schemes based on elastomers can be chosen as required. The application of elastomers also expands the range of printing material options for 4D implants.

The 4D deforming procedures can also be powered by a pre-stored stress field in the driving layer. By distributing phase-changing wax microparticles (MPs) in one elastomer layer (none in the other layer), the heating-pre-stretching-cooling process endowed it with a pre-strained shape (Figure 3Ad). Once heated again, the liquid–solid-phase change of wax MPs released the pre-stored stress, and the shape returned^[84]. This study tactfully utilized the phase

transition of wax MPs to store and release pre-strain. Our previous study proposed a UV-sensitive hydrogel-based self-bending structure by pre-storing strain in the driving layer based on a reversible ionic bond between carboxyl groups and exogenous ferric ions^[85]. The result shows that reversible ionic crosslinking in hydrogels can also realize pre-stress storage. Hagaman *et al.* designed a double-layer actuator driven by light. The driving layer was photoactive, and once irradiated by appropriate wavelength light (such as UV light and blue light), a trans-cis isomerization of the AB molecules occurred inside, thus generating stress and actuating curving deformation^[86]. The study presents an easy method that generates inner stress by transforming internal conformation under the stimulus. Differences in internal stresses in bilayer constructs drive them to

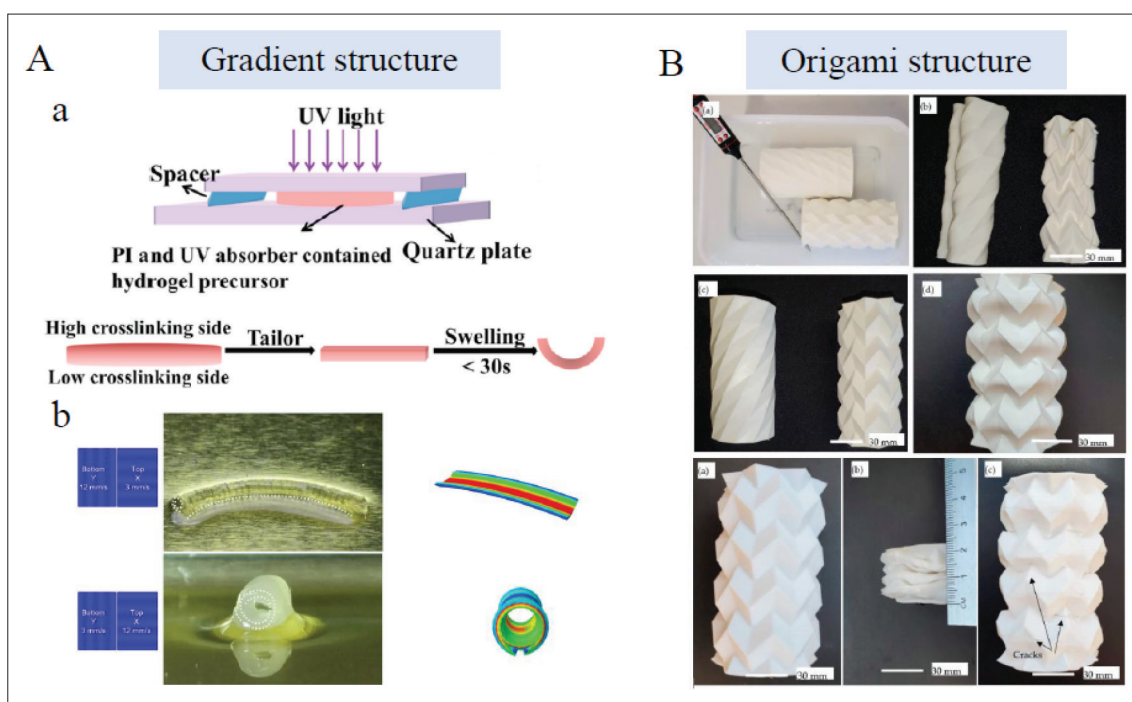


Figure 4. Gradient and origami structure design in 4D printing. (A) Gradient structural design, a) Crosslinking gradient in a photocuring hydrogel formed under UV light due to the different distance to light source^[91]. Copyright 2022, Elsevier. b) Graded structures based on LCEs by means of regulating printing parameters (such as printing speed, and printing direction)^[92]. Copyright 2020, American Chemical Society. (B) Origami structural design, origami structures for minimally invasive surgeries with high recovery^[103]. Copyright 2021, MDPI. PI: Photoinitiator.

bend, curve^[86], and then form a helix^[87]. Though these deformations are internally driven by internal stress, we attribute them to these categories because their external actuation is light, heat, and some other stimulus.

Based on these design principles, shape-morphing behaviors are initiated in multi-layer structures. As shown in Figure 3B, Ding *et al.* designed a trilayer structure consisting of two outer oxidized methacrylated alginate layers with different swelling and degradation capacities and a GelMA layer. Due to the anisotropic swelling of the three layers and degradation of the fast-degradation layer, the structure underwent five phases of deformation. More interestingly, due to reversible ionic crosslinking, the remaining double-layer structure can deform reversibly in calcium ions (Ca^{2+}) and tetraacetic acid, respectively^[88,89].

More complex programmed deformation (such as local buckling, curling, etc.) can be achieved through partial pattern design in the printing of bi-/multi-layer strips^[81,84,85]. In these driving designs mentioned above, finite element analysis (FEA) simulations are conducted to predict shape transformations which can effectively calculate the effect of each parameter on shape morphing according to mathematical models based on deformation mechanisms^[76,84].

Through bi-/multi-layer design, self-bending, self-rolling, and self-buckling structures activated by moisture, light, pH, and so forth can be easily prepared. This establishes a foundation to utilize 4D-printed implants to repair lumen organs such as vessels, trachea, intestines, and organs with a curved surface topology such as the heart and others. The range of materials available for the preparation of 4D printing implants has also been widened to the elastomer, which supports the generation of implants with higher toughness and strength when necessary. Meanwhile, the fabrication of multi-layer structures permits the reconstruction of complex biological tissues.

4.2.2. Gradient structure design

The formation of gradient structures has great prospects in the production of 4D programmed scaffolds. It facilitates the 4D deformation of single-layer structures. For photocuring bioinks, crosslinking density attenuates with the increase of distance along the light irradiation path in the presence of a photoinitiator and ultraviolet absorber. Thus, the gradient in crosslinking density can be created. The upper portion of hydrogel closest to a light source presents higher crosslinking density, while the lower part presents a lower crosslinking degree. Under this circumstance, the resultant anisotropic swelling induces inner strain that prompts deformation^[12,90,91] (Figure 4Aa). For SMPs and

LCEs, the 4D transformation of gradient structures can be programmed by regulating printing parameters. Adjusting printing speed, printing path, and part geometry drives their deformation patterns by graded thermal distribution in a specific direction^[92,93] (Figure 4Ab). The generation of gradient structures broadens the design space of 4D deformation constructs and has wide application prospects in the field of tissue engineering.

4.2.3. Origami structure design

Origami structures have extended their application in the biomedical field owing to their self-deployment ability, which can expand from a small-sized volume to a larger functional device. Despite the difficulties in fabricating their complex configurations, the emergence of 4D printing technology reduces manual pressure and facilitates the process. The folding modes are of great importance in origami-derived objects so they can be designed to fold and unfold transversely or longitudinally. The collapsible objects can be divided into a series of repeated foldable elements. Different flexible folding processes can be achieved by designing these sub-units and nearby creases. The choice of materials for these constructs mostly relies on SMPs that enable them to respond to thermal stimulation. The PLA stents formed by square elements and helical angles were built to self-deploy in large shrinkage ratios^[94]. Triangular^[95], hexagon^[96], honeycomb^[97], and hinge^[98]-shaped sub-units were also adopted in the deployable and reconfigurable structures. It is noteworthy that Manen *et al.* designed different types of unit cells by regulating the printing path to form various origami-like deformed supports^[99]. Different folding structures are produced through the design of creases, such as connecting SMP to an elastomeric matrix at the crease^[100] or programming precisely the local gradients in hydrogels by modifying irradiation direction and time of ultraviolet light^[101]. Furthermore, by printing designed patterns on pre-stretched substrates, complex origami structures mimicking a butterfly, the Sydney Opera House, a rose, and a dress with poly (dimethylsiloxane)-based elastomer as materials were made^[102]. It can thus be seen that various complex deformation processes can be realized through origami design. On this basis, origami structures for minimally invasive surgeries with high recovery have been created (Figure 4B)^[103]. The generation of origami structures enriches the deformation effect in 4D printing. The programmability, agile deformability, and self-assembly property position the origami structures as promising devices in a medical application^[99,103,104]. It is of great application significance for minimally invasive surgery to design origami structural implants that match targeted organs or tissues as required. They can be implanted in the folded state and deploy automatically after being implanted.

5. Application

From first proposed in a TED talk^[105] to subsequent development, 4D printing brings great possibilities for tissue replacement, restoration, and medically implanted devices in biomedical fields. It is a huge step forward following 3D printing, and it offers special advantages including but not limited to (i) convenience in the implantation of minimally invasive surgery due to flexible shape transformation; (ii) seamless fit with defected tissues owing to programmed shape-morphing process after implanted; (iii) formation of bionic structures, and dynamic deformation conducive to cell adhesion, proliferation, and differentiation; (iv) realization of biomimetic behaviors in body tissues such as joint activity, muscle contraction, and relaxation; and (v) responsiveness to a physiological condition such as pH, body fluid, temperature, biochemicals, etc. This section summarizes the application procedure of 4D-printed implants *in vivo* (Figure 5). Then, we focus on the interaction of 4D printing scaffolds with cells (Table 1) and the application of 4D-printed representative implants (Table 2).

5.1. Application procedure

To apply 4D-printed implants *in vivo* on tailor-made conditions, pre-modeling steps that detect anatomical structures of diseased sites with the assistance of clinical imaging information are needed first^[106]. On this basis, implants are designed, and operational procedures are planned^[107] to allow the selection of optimized implantation approaches and subsequent deformation programming before surgical intervention.

The deformation programs can be divided into two types: (i) performing stimulus-responsive deformation in advance and then implanting *in vivo*^[76]; (ii) initiating *in situ* deformation after implantation^[108]. The former applies to the fabrication of some tubular and curved implants, including tracheal^[76], vascular^[109], intestinal implants^[85], cardiac patches^[110], and more. Biomedical implants conforming to specific physiological bending degrees can be obtained as required through pre-programming and following stimulus-responsive deformation. 4D printing technology provides faster, more intelligent, and more accurate preparation during this process. Potential stimulus needed in the procedure can be easily acquired *in vitro*. The latter has huge application value for minimally invasive surgery and all regular or irregular tissue defects repair. Since it deforms after being implanted *in vivo*, the stimulation conditions are limited to physiological stimulus *in vivo*^[111] and remote stimulus *in vitro*^[112]. The body possesses a diverse physiological environment, and there are a variety of stimulation conditions that can drive

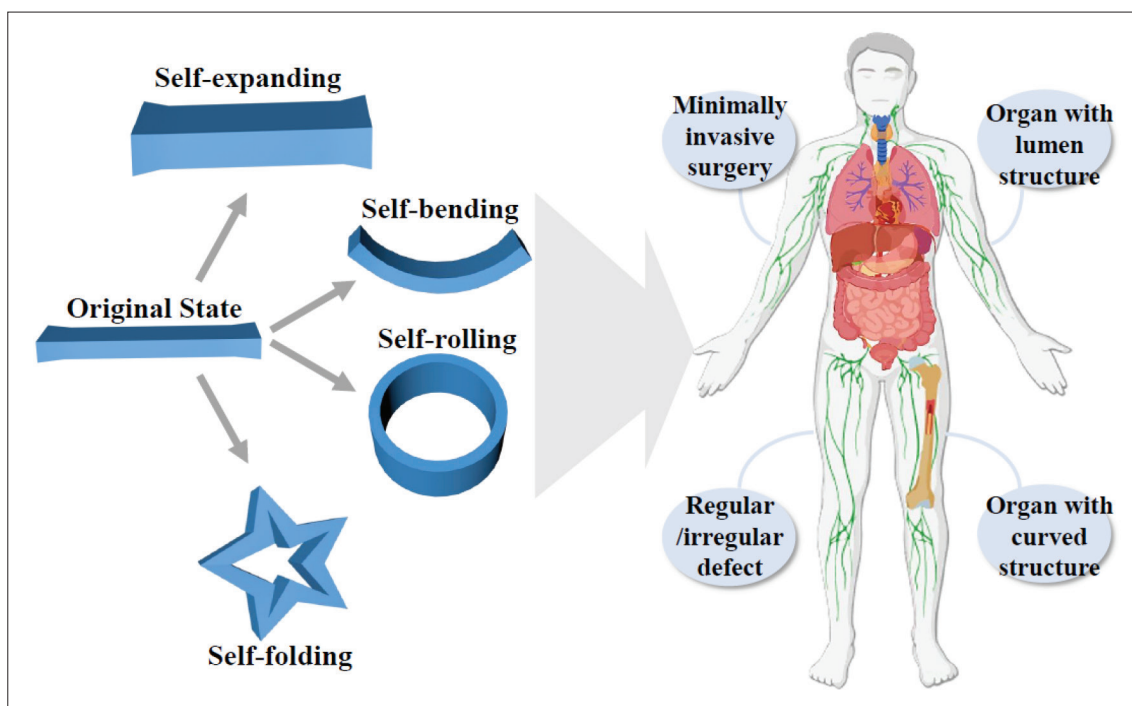


Figure 5. The application of 4D-printed implants in the body.

structural 4D changes, including body fluid, temperature, pH, biochemicals, and more^[23]. Specifically, the design of smart implants responsive to humoral stimulation mainly depends on anisotropic swelling characteristics within the entire structure, as mentioned. Body temperature is around 37°C. Materials that respond to body temperature include SMPs, PNIPAM hydrogel, and others. Some studies have explored SMPs with shape transition temperatures close to body temperature, such as poly (glycerol dodecanoate) acrylate (PGDA)^[111] and polyurethane using a specific synthesis method^[113]. Intravascular implants thus obtained show satisfactory deformation effects *in vitro* devices or *in vivo* environments. Gastric and intestinal juice present different pH values, and the pH-induced deformation depends on different swelling behaviors of hydrogels under acidic or alkaline conditions^[23]. For example, researchers used a type of hydrogel containing a large number of carboxyl groups on the side chain, and high and low swelling properties under alkaline and acidic conditions are caused due to ionization and deionization effects under different pH conditions. Thus, pH-driven expansion, contraction, and torsion can be achieved^[114]. Biochemical signals are an important part of dynamic environments *in vivo*. The exploration of biochemical-sensitive implants is thus a research focus. Concerning this, researchers have prepared a glucose-responsive hydrogel network. High glucose concentration can affect the crosslinking density of the micronetwork,

thus promoting the release of encapsulated insulin, further promoting the healing of diabetes wounds^[115]. In addition, extracorporeal remote stimulus (including magnetism^[112,116], light, local temperature^[108], etc.) can also induce 4D deformation after implants are implanted into the body.

All in all, basic models of different implant sites can be obtained according to clinical imaging, and then smart implants are pre-programmed to meet the needs of implantation sites. Relying on external and internal stimulation, 4D deformation of implants can be realized both before and after they are implanted into the body, which can satisfy intelligent adaptive repair and replacement of different tissue defects.

5.2. 4D printing cellular scaffolds

There are two types of 4D printing scaffolds with cells: cell-laden scaffolds and cell-seeding scaffolds. The cell-laden scaffolds are defined as synchronous 4D printing of biomaterials and cells. Commonly used biomaterials contain gelatin, GelMA, collagen, alginate, poly (ethylene glycol) (PEG), de-cellularized extracellular matrices (dECMs), and others. The physicochemical properties of these 4D dynamic materials can be modulated by external stimulus over time and act as guidance on the behavior of embedded cells^[117,118] to reconstruct dynamic natural cellular microenvironments^[119]. For example, protein-polymer hydrogel biomaterials prepared by Liu *et al.*

Table 1. 4D printing cellular scaffolds.

Category	Ink compositions	Cell	Fabrication methods	Stimuli	Possible applications	References
Cell-laden scaffolds	Oxidized and methacrylate alginate (OMA)	Human mesenchymal stromal cells (hMSCs)	DIW	Solvent	Cartilage-like tissue	[90]
	Hyaluronan, alginate	hMSCs	Extrusion-based printing	Solvent	Cartilage-like tissue	[122]
Cell-seeding scaffolds	Collagen	Fibroblasts	Laser-assisted bioprinting	Stress-release contraction	Soft tissue engineering	[121]
	Gel-MA, Gel-COOH-MA	Human umbilical vein endothelial cells (HUVECs)	Inkjet printing	Solvent	Mimicking microvessels	[109]
	Polyurethane	hMSCs	FDM	Temperature	Scaffolds for tissue engineering	[124]
	SMP	Neural stem cells (NSCs)	FDM, extrusion-based printing, stereolithography	Temperature	Culture substrates	[126]

that underwent 4D cyclic mechanical loading proved to have an influence on fibroblast-to-myofibroblast transdifferentiation^[120]. Moreover, Douillet *et al.* presented a novel model via laser-assisted bioprinting (LAB) to make a replication of fibroblast dynamic remodeling *in vitro*^[121]. This method can be utilized to understand better cellular behaviors and interactions with the extracellular matrix (ECM). Except for these studies that affect cells through the regulation of internal networks, some researchers use cell-laden 4D bioprinting to form cartilage-like tissue^[90,122] and vascularized tissue^[123], which are quite meaningful to tissue/organ regeneration applications.

The cell-seeding scaffolds refer to culturing cells on printed scaffolds directly. Dynamic platforms or scaffolds are prepared via 4D printing of biomaterials (Figure 6A and B), and it is demonstrated that their time-dependent deformation influences cell morphology^[124] and regulates cell behaviors, including adhesion, proliferation^[125], and differentiation in spatiotemporal control^[126], and further controls cell functions^[127]. Cui *et al.* encapsulated human umbilical vein endothelial cells (HUVECs) in self-folded microtubes that deformed by swelling difference of two layers to mimic microvessels, which resembled the ECM in body tissues and promoted cell adhesion, spreading, and proliferation^[109]. They also predicted the application prospects of engineering tissues in this structure, as shown in Figure 6C. These values offer instructive guidance for creating cell culture platforms and scaffolds resembling native ECM functions.

5.3. Tissue engineering

5.3.1. Bone scaffolds

4D printing has been widely applied to bone defects. The 4D-printed bone scaffolds allow minimally invasive implantation and fit irregular bone defects perfectly^[23]. Mechanical properties, porosity, degradation rate, and biocompatibility of bioscaffolds are of great importance to implantation *in vivo* for bone tissue engineering. Thermo-responsive SMP composites are mostly used to fabricate bone scaffolds^[116,128,129]. For instance, Zhang *et al.* presented bone tissue-like structures printed by PLA/Fe₃O₄ composite filaments via FDM printer with shape memory effect of both heat- and magnetic-induced actuation (Figure 7A)^[116]. In addition, various bioactive substances have been introduced to SMP scaffolds to enhance osteogenic activities, such as hydroxyapatite (HA)^[130,131], bioactive glasses^[132], and others. Furthermore, remote regulation of stem cell fate can be realized by 4D programming in bone repair. You *et al.* utilized 4D printing technique to fabricate a multi-responsive bilayer morphing membrane consisting of an SMP layer and a hydrogel layer (Figure 7B)^[108]. Once implanted in the bone defect, the membrane can morph due

Table 2. Applications of 4D-printed representative implants.

Applications	Ink compositions	Fabrication methods	Stimuli	Deformation principle	References
Bone repair	Chitosan (CS) reinforced poly-lactic-acid (PLA)	Fused filament fabricated (FFF)	Temperature	Shape memory effect of SMPs	[129]
	Poly (D,L-lactide-co-trimethylene carbonate)	Extrusion-based printing	Temperature	Shape memory effect of SMPs	[130]
	Poly (ε-caprolactone)-diacrylates (PCLDA)	DLP	Solvent, temperature	Anisotropic swelling behavior and shape memory effect of SMP	[108]
	PLA/Fe ₃ O ₄	FDM	Temperature, magnetic field	Shape memory effect of SMPs, and addition of magnetic particles	[128,166]
Vascular stents	Polyurethane	FDM	Temperature	Shape memory effect of SMPs	[104]
	PLA	FDM	Temperature	Shape memory effect of SMPs	[60]
	Poly (glycerol dodecanoate) acrylate (PGDA)	Extrusion-based printing	Temperature	Shape memory effect of SMPs	[111]
	s-PCL	UV light-assisted 3D printing	Temperature	Shape memory effect of SMPs	[135]
	PLA	FDM	Temperature	Shape memory effect of SMPs	[30]
Vascular repair devices	Urethane diacrylate and semi-crystalline polycaprolactone (PCL)	DIW	Temperature	Shape memory effect of SMPs	[136]
Cardiac defect	PLA-MNCs	FDM	Temperature, magnetic field	Shape memory effect of SMPs, and addition of magnetic particles	[139]
	PLA-Fe ₃ O ₄ nanoparticles	FDM	Temperature, magnetic field	Shape memory effect of SMPs, and addition of magnetic particles	[112]
	Polyethylene glycol (PEG)/PLA	FDM	Temperature	Shape memory effect of SMPs	[140]
Cardiac patches	A shape memory polymer and graphene	DLP	Temperature, near-infrared (NIR) light	Shape memory effect of SMPs, photothermal conversion capacity of graphene	[110]
Tracheal stent	Bi-layered Sil-MA hydrogels	DLP	Solvent	Anisotropic swelling behavior	[76]
	Polypropylene glycol/polycaprolactone triblocks	DLP	Temperature	Shape memory effect of SMPs	[144]
	Methacrylated polycaprolactone	SLA	Temperature	Shape memory effect of SMPs	[145]
	PLA/Fe ₃ O ₄	FDM	Magnetic field, infrared light	Addition of magnetic particles, photothermal capacity of infrared light	[146]
	PLA/Fe ₃ O ₄	FDM	Magnetic field	Addition of magnetic particles	[147]
	PLA/PCL	DIW	Temperature	Shape memory effect of SMPs	[148]
Brain model	SMP and graphene	Extrusion-based printing	NIR	Photothermal conversion capacity of graphene	[150]

Nerve regeneration	Reduced GO, mesoporous silica, and a thin carbon layer	DLP	Magnetolectric	Magnetolectric conversion of materials	[152]
Skeletal muscle mimetic tissue	Soybean oil epoxidized acrylate (SOEA)	SLA	Solvent	Internal-stress-induced transformation	[33]
	Polyvinyl alcohol (PVA), PCL and PLA coating, SOEA coating	FDM	Temperature	Shape memory effect of SMPs	[31]
Intestine repair	Gelatin methacryloyl (GelMA), gelatin	Electrically-assisted extrusion-based printing	Solvent	Anisotropic swelling behavior	[149]
	Acrylamide-acrylic acid/cellulose nanocrystal	Extrusion-based printing	UV light, solvent	Anisotropic shrinkage and swelling behavior	[85]
Orbital stent	PTU, gold nanoparticles, nano-hydroxyapatite	Extrusion-based printing	Temperature	Shape memory effect of SMPs	[153]
Drug delivery	AAc, N-isopropylacrylamide, PVP	Femtosecond laser direct writing	pH	Different swelling behavior in alkaline and acid solutions	[114]
	Zein gel	Extrusion-based printing	Solvent	Porosity influenced by hydrophobic attraction	[157]
	Poly (N-isopropylacrylamide) (PNIPAM)	Extrusion-based printing	Temperature	Thermo-responsive characteristics of material	[155]

to the swelling behavior of the hydrogel layer to conform to the complex geometry of tissue defect. Then, external heating was introduced to activate responsive surface microstructures in the SMP layer to precisely meet the needs during different phases in proliferation and differentiation, thus promoting the bone formation. This shows that 4D printing dynamic bone implants can complete structural and even deeper functional repair of bone defects.

5.3.2. Cardiovascular stents

4D-printed devices have great potential for the treatment of various cardiovascular diseases because the cavity structures of vascular lumens can be easily obtained by the self-rolling process of 4D constructs^[133]. Specifically, 4D programming stents produce a marked effect in thrombus, vascular stenosis, and others. Shape memory stents based on SMPs, including poly (glycerol dodecanoate) acrylate- (PGDA-) [111], PLA-[30,60], and PCL-based^[134-136] composites and hydrogels, including pNIPAM-based composites^[137], were fabricated for adaptive vascular implantation. They possess good self-expanded behavior under thermal stimulation close to body temperature, in which condition shape programming at room temperature and subsequent shape deployment *in vivo* can be realized (Figure 8A). Besides, origami-inspired bifurcated stents using Polyurethane as material were also created for the treatment of stenosis and obstruction in Y-shaped branched vessels (Figure 8B)^[104]. 4D-printed self-rolling structure for vascular tissue engineering has also been widely explored. Kirillova *et al.* utilized gradient structure design to fabricate 4D-printed hollow self-rolling tubes with an average inner diameter of 20 μm, equivalent to the minimum vessel diameter, to mimic microvascular tissue, which was not achieved by other existing biofabrication methods^[12].

Unlike tubular vascular substitutes or stents, the heart surface presents a curved topological structure with arranged myocardial cells. 4D printing can also be utilized to produce cardiac patches that conform to physiological surfaces through pre-programming and mechanical stimulation. Currently, researchers have made efforts to make smart cardiac patches for the treatment of myocardial infarction (MI)^[110,138] and atrial fibrillation (AF)^[139]. For example, 4D-printed NIR light-sensitive cardiac constructs with highly aligned myofibers and adjustable curvature were produced to treat MI^[110]. It can mimic and reconstruct the curved topology of myocardial tissue to realize seamless integration. Meanwhile, a uniform distribution of aligned cells and excellent myocardial maturation on 4D-curved cardiac constructs were observed (Figure 8D). Beyond these, 4D-printed thermo-responsive SMP stents can be used for the repairment of cardiac defects, such as ventricular

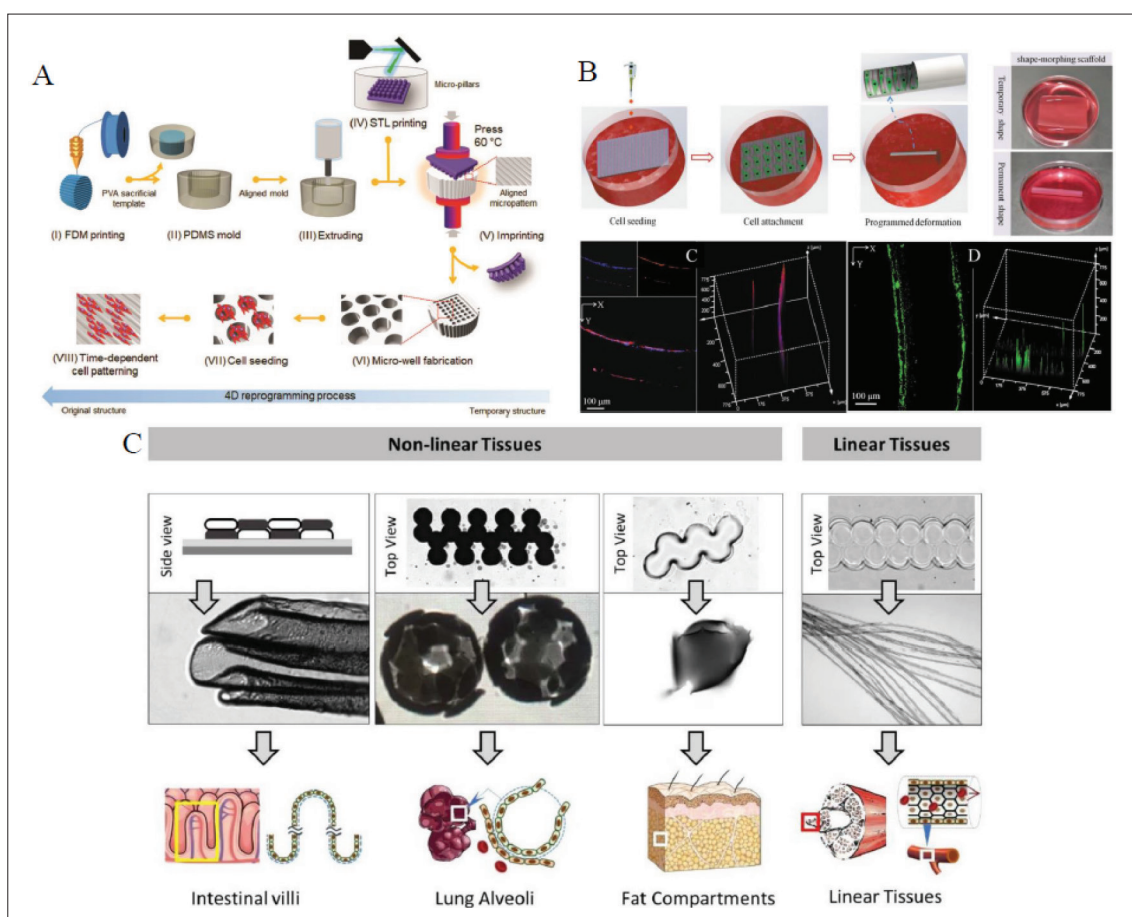


Figure 6. 4D printing cell-seeding scaffolds. (A) The fabrication procedure of a 4D platform with a time-dependent topographic transformation^[126]. Copyright 2020, Wiley-VCH. (B) The preparation of 4D scaffold with tubular structure and 3D cell organization^[125]. Copyright 2020, Wiley-VCH. (C) Self-folded cell-seeding microstructures designed with different layouts and patterns have great potential for different tissue-engineering applications^[109]. Copyright 2020, IOP Publishing.

septal defect (VSD)^[140] and atrial septal defect (ASD) (Figure 8C)^[112].

5.3.3. Tracheal stents

Trachea is an important air conduit connecting the larynx to the carina with the function of ventilation, secretion removal, and keeping the airway unobstructed^[141]. It is fragile and can be damaged by many disorders^[142]. Trachea stents are an effective treatment for maintaining airway patency^[143]. Due to its natural tubular structure, 4D printing can be a potential approach to make trachea-like stents for the treatment of tracheal injury and airway stenosis. SMP-based custom-made endotracheal stents are presented in several studies^[144-148]. Maity *et al.* described a personalized tracheal stent based on photopolymerizable inks containing polypropylene glycol/polycaprolactone triblocks using a DLP-based 3D printer^[144]. The stent demonstrated great shape memory behavior for safer implantation. *In situ* welding strategy was also developed

firstly for further reduction of the insertion profile of the stent. Ciprofloxacin was added into the ink, which was released *in vitro* over time and endowed the stent with antimicrobial activity to prevent implant-related infections. This shows that 4D-printed implants are feature-rich after design and function well for tracheal defects. Shape-morphing hydrogels are also utilized for tracheal reconstruction. Kim *et al.* presented a bi-layered Sil-MA hydrogel based on digital light processing (DLP). The 4D deformation depended on the anisotropic volume change of the bi-layered hydrogel in an aqueous solution. Then curved trachea mimetic tissue was made equipped with two types of cells, and performed well in tracheal injury of rabbits (Figure 9A)^[76].

5.3.4. Other organs

In addition to these typical applications mentioned above, 4D printing has also demonstrated application value in bionic artificial muscle^[31,149], brain model^[150,151], neuronal

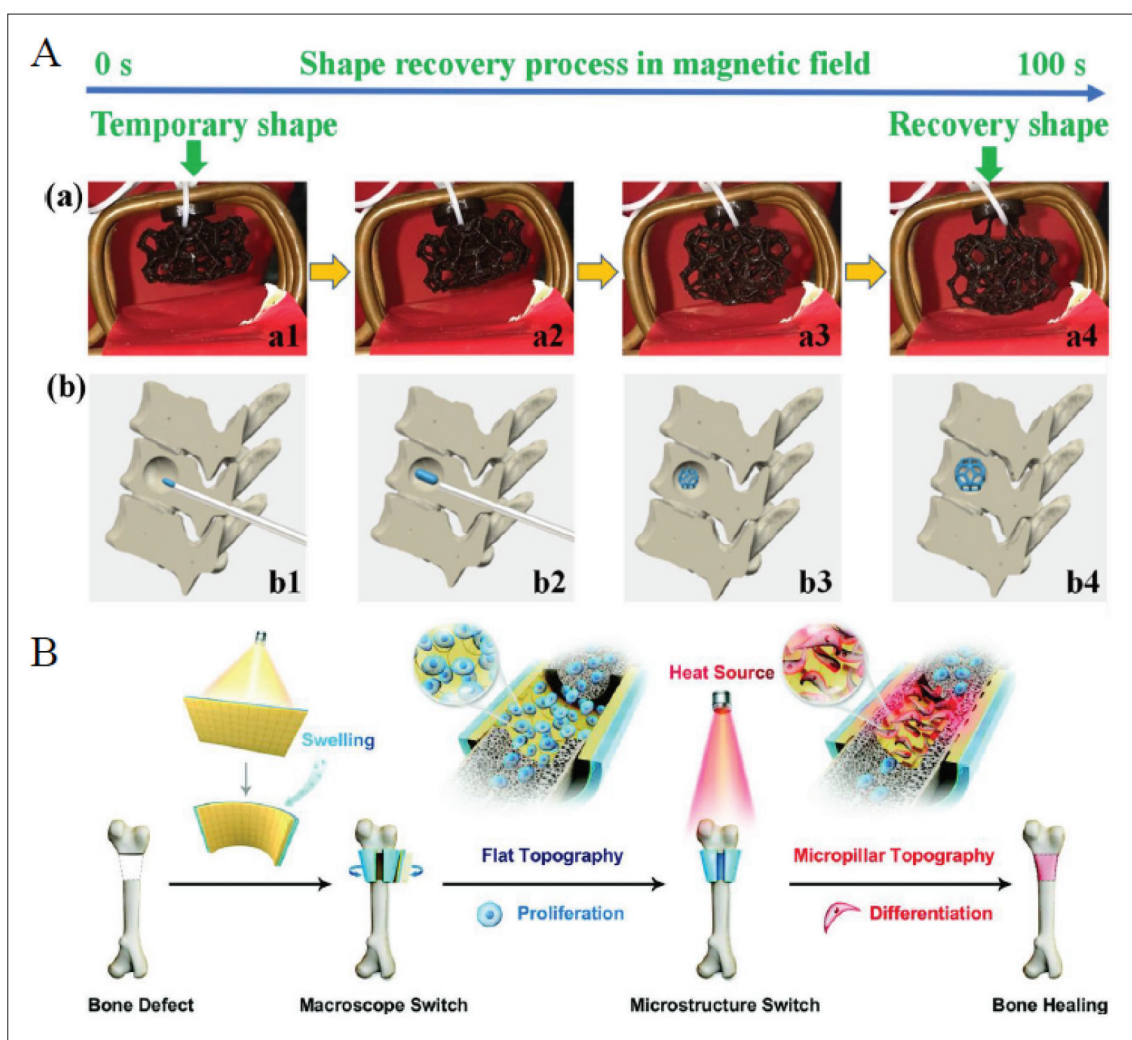


Figure 7. Application of 4D printed in bone defects. (A) Shape recovery behavior of the 4D-printed structure in a magnetic field and their application for bone repair^[116]. Copyright 2019, Elsevier. (B) A functional multi-responsive bilayer morphing membrane used for bone repair and bone formation^[108]. Copyright 2021, Wiley-VCH.

regeneration^[33,152], intestinal defect repair^[85], enophthalmic invagination^[153], and others (Figure 9B–D). By implanting 4D dynamic scaffolds in minimally invasive therapy, *in situ* damage to tissues can be avoided, which greatly improves the post-operative comfort of patients^[154]. Meanwhile, 4D implants can conform to irregular tissue defects perfectly. Besides, 4D printing is able to reconstruct some cavities or parenchyma organs dynamically. 4D-printed implants show great potentials in tissue restoration and reconstruction, and promote significant progress for tissue engineering.

5.4. Drug delivery

There are two methods to deliver drugs in 4D-printed implanted devices. One is to add targeted drugs in the initial bioink^[144], and drugs can release after scaffold

implantation. This method is simple, but the drug release rate is difficult to control, and intelligent on-demand release cannot be achieved. Another way is to design intelligent polymer networks or deformable devices with 4D printing. They can be actuated by physiological stimulation *in vivo* or remote stimulation *in vitro* after being implanted to release drugs autonomously and controllably. For example, Zu *et al.* designed a bioinspired smart hydrogel capsule via extrusion-based 4D printing, consisting of UV crosslinked PNIPAM hydrogel as the shell and drugs as the core (Figure 10A). The drugs can release controllably based on the ambient temperature, and the release profile can be modified by adjusting the internal pore size of hydrogel capsules^[155]. The 4D-printed core-shell structure is an applicable device to deliver drugs on demand^[156]. Hu *et al.* reported a pH-responsive

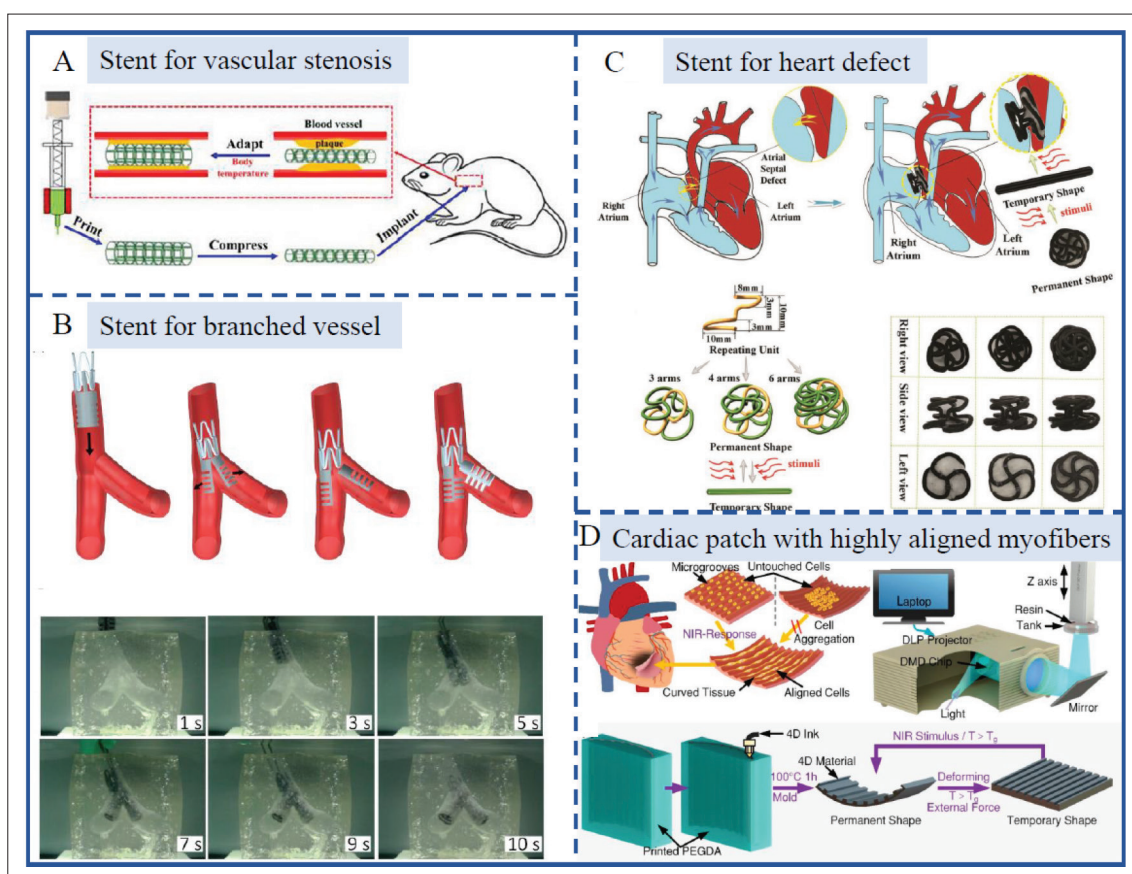


Figure 8. Application of 4D-printed scaffolds in cardiovascular diseases. (A) Self-expanded stent for vascular stenosis.^[111] Copyright 2021, Elsevier. (B) The deforming procedures of the folded stent inserted into the branched blood vessels.^[104] Copyright 2019, Jove publishing. (C) 4D-printed shape memory occlusion for atrial septal defect (ASD).^[112] Copyright 2019, Wiley-VCH. (D) A 4D-printed NIR light-sensitive cardiac patch with highly aligned myofibers for the treatment of myocardial infarction (MI).^[110] Copyright 2021, American Chemical Society.

hydrogel printed by femtosecond laser direct writing at the microscale in another study. They designed a complex microcage to capture and release microparticles due to the different pore sizes in the expanded and contracted states, showcasing its possibility in drug delivery (Figure 10B)^[114]. Utilizing the change of polymer network pore size to release drugs dynamically as required is also an efficient method^[157]. By empowering implants with the ability of drug delivery, post-implantation infections can be prevented by antibiotics, primary diseases of implantation sites can be treated by therapeutic drugs, and diseased tissues can be repaired by growth factors or other functional components. With the assistance of 4D printing, the drug delivery system can achieve more effective drug administration that delivers drugs on demand. It is expected to combine bioscaffolds with tunable functional drug delivery by 4D printing design, which can realize the combination of dynamic repair and dynamic drug administration for promotion of further rehabilitation.

6. Conclusion and perspectives

Overall, 4D printing is a potential candidate technology in producing dynamic and functional scaffolds for medical implantation. It developed from 3D printing and has made great progress in generating time-dependent drivable constructs when exposed to specific stimuli instead of traditional static structures. The 4D-printed scaffolds based on structural deformation demonstrate great advantages in minimally invasive surgery due to their small to large volume transformation under stimulation, thus reducing intraoperative risk and improving patient prognosis. Meanwhile, they can be programmed to fit perfectly to tissue defects by self-deforming after implanted. 4D printing has great advantages in producing implants and substitutes with specific shapes. Tubular and curved implants can be easily achieved through self-rolling and self-bending, which are hardly achievable by the traditional manufacturing process. The 4D-printed cellular

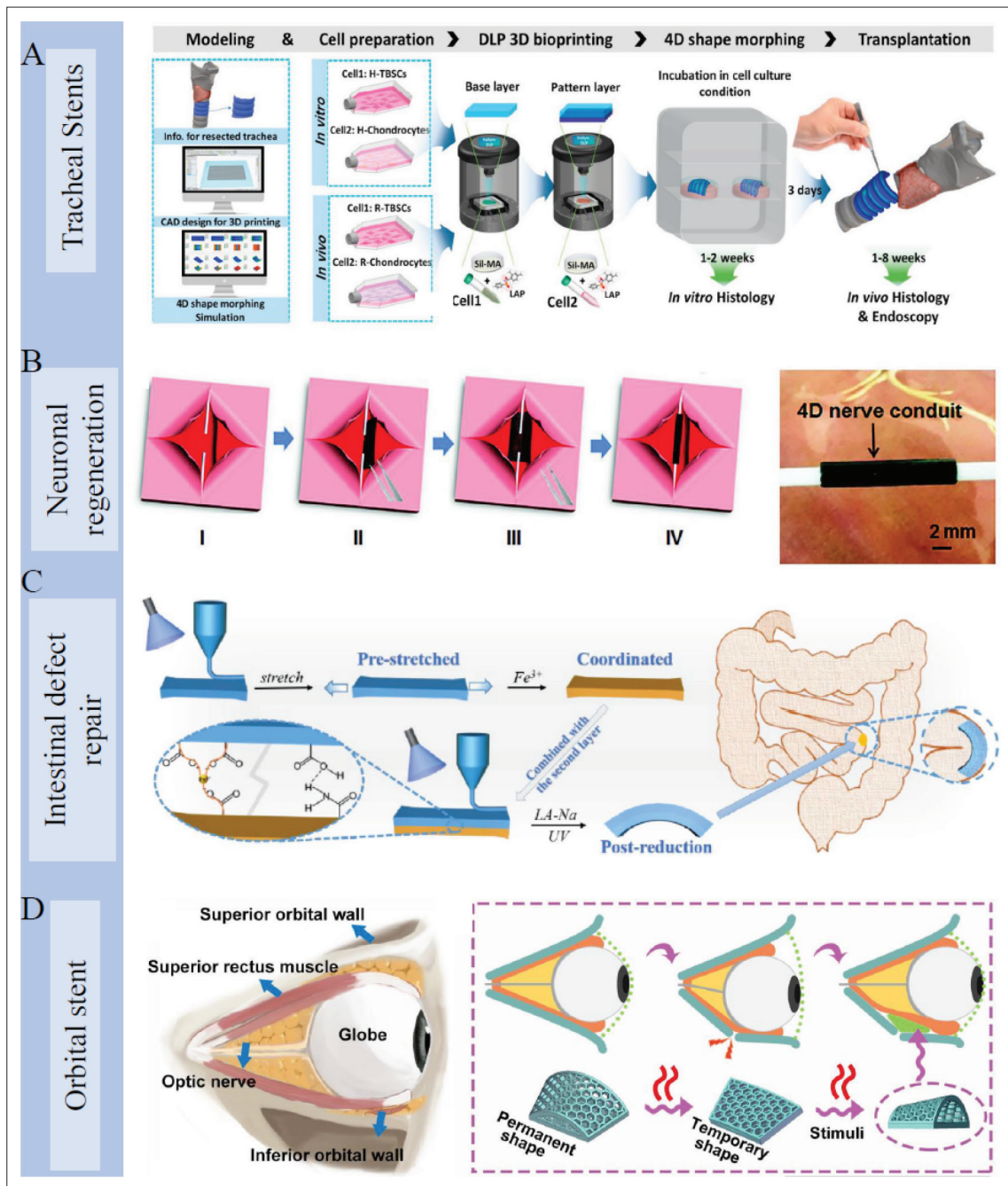


Figure 9. Application of 4D-printed scaffolds in various organs. (A) Manufacturing process of 4D-printed self-curved tracheal stent for *in vitro* and *in vivo* study^[76]. Copyright 2020, Elsevier. (B) 4D nerve guidance conduit for neural engineering^[33]. Copyright 2018, Wiley-VCH. (C) A 4D-printed bilayer hydrogel with adjustable bending degree for intestinal defect repair^[85]. Copyright 2022, Elsevier. (D) A 4D-printed orbital stent for the treatment of enophthalmic invagination^[153]. Copyright 2022, Elsevier.

scaffolds shift the emphasis toward generating mimetic ECM structures that interact with contacted cells, which expands the source possibility of tissue/organ grafts and substitutes. Combined with clinical imaging, 4D printing smart implants have a wide foreground in

the medical field for their ability to realize personalized adaptive implantation through pre-programming.

Though 4D-printed implants have shown a huge application prospect and inspired much creative research, they are still in the initial stage and facing many

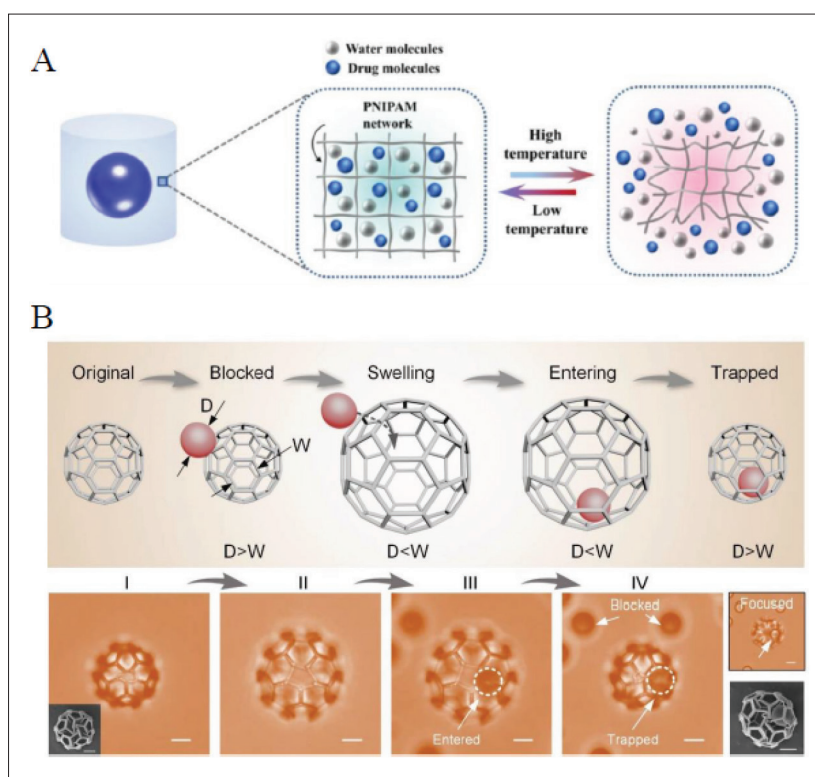


Figure 10. 4D-printed drug delivery devices. (A) 4D-printed core-shell structure consisting of UV crosslinked PNIPAM hydrogel as the shell and drugs as the core for controlled drug release^[155]. Copyright 2022, Elsevier. (B) A pH-responsive microcage for the capture and release of microparticles due to the different pore sizes in the expanded and contracted states^[114]. Copyright 2019, Wiley-VCH. PNIPAM: poly (N-isopropylacrylamide).

challenges. Firstly, available biomaterials are limited; more materials with stimuli-responsive properties or existing materials with the potential for 4D structure formation should be exploited. Biocompatibility and biodegradability of materials used need to be considered. Degradation products of these materials, which are often overlooked in previous studies, should be tested via both *in vivo* and *in vitro* experiments to ensure that they are harmless to the body as well. In addition, implant infection must be prevented by design, such as coating implants during design, adding antibacterial agents in the printing ink, and others. Secondly, printing technologies remain to be updated in order to implement multi-materials, high-speed, and high-resolution 4D printing. Additionally, more response conditions related to the internal environment, as well as non-contact response conditions are required to explore continually to expand application of 4D scaffolds *in vivo*. Meanwhile, reversibility and repeatability of stimuli-responsive deformation of scaffolds need to be achieved as different application condition requires. Finally, for the sake of personalized medical treatment, imaging information of defect tissues, corresponding modeling, subsequent programming of 4D scaffold, and deformation after

implantation are all closely interlinked. Therefore, the accuracy of clinical imaging, development of modeling software, controllability of deformation programming, and development of the particular software to pre-simulate deformation *in vivo* all need to take effort to reach.

The 4D-printed implants have the ability to self-deform in response to multiple physiological and extracorporeal signals, and they are quite instructive for biomedical applications. It still requires multi-disciplinary cooperation to promote produced dynamic scaffolds from laboratory investigation to clinical practice.

Acknowledgments

None.

Funding

This work was supported by National Natural Science Foundation of China (82270595, 32171402), the China Postdoctoral Science Foundation (BX20220393, 2022M723891), Key Research and Development Program of Jiangsu Province (BE2022823, BE2021727),

and Jiangsu Provincial Medical Innovation Center (CXZX202217).

Conflict of interest

The authors declare no conflicts of interest.

Author contributions

Conceptualization: Jianan Ren, Xiuwen Wu, Zongan Li, Jinjian Huang, Guiwen Qu

Supervision: Jianan Ren

Visualization: Guosheng Gu

Writing – original draft: Guiwen Qu

Writing – review & editing: Jinjian Huang

Ethics approval and consent to participate

Not applicable.

Consent for publication

Not applicable.

Availability of data

Not applicable.

Reference

1. Liu G, He Y, Liu P, *et al.*, 2020, Development of bioimplants with 2D, 3D, and 4D additive manufacturing materials. *Engineering*, 6(11): 1232–1243.
<https://doi.org/10.1016/j.eng.2020.04.015>
2. Dixon DT, Gomillion CT, 2022, Conductive scaffolds for bone tissue engineering: Current state and future outlook. *J Funct Biomater*, 13(1): 1.
<https://doi.org/10.3390/jfb13010001>
3. Cockerill I, See CW, Young ML, *et al.*, 2021, Designing better cardiovascular stent materials: A learning curve. *Adv Funct Mater*, 31(1): 2005361.
<https://doi.org/10.1002/adfm.202005361>
4. Teo AJT, Mishra A, Park I, *et al.*, 2016, Polymeric biomaterials for medical implants and devices. *ACS Biomater Sci Eng*, 2(4): 454–472.
<https://doi.org/10.1021/acsbiomaterials.5b00429>
5. Azlin MNM, Ilyas RA, Zuhri MYM, *et al.*, 2022, 3D printing and shaping polymers, composites, and nanocomposites: A review. *Polymers*, 14(1): 180.
<https://doi.org/10.3390/polym14010180>
6. Sonatkar J, Kandasubramanian B, Ismail SO, 2022, 4D printing: Pragmatic progression in biofabrication. *Eur Polym J*, 169: 111128.
<https://doi.org/10.1016/j.eurpolymj.2022.111128>
7. Osouli-Bostanabad K, Masalehdan T, Kapsa RMI, *et al.*, 2022, Traction of 3D and 4D printing in the healthcare industry: From drug delivery and analysis to regenerative medicine. *ACS Biomater Sci Eng*, 8(7): 2764–2797.
<https://doi.org/10.1021/acsbomaterials.2c000942764>
8. Li Y-C, Zhang YS, Akpek A, *et al.*, 2017, 4D bioprinting: The next-generation technology for biofabrication enabled by stimuli-responsive materials. *Biofabrication*, 9(1): 012001.
<https://doi.org/10.1088/1758-5090/9/1/012001>
9. Huang J, Xia S, Li Z, *et al.*, 2021, Applications of four-dimensional printing in emerging directions: Review and prospects. *J Mater Sci Technol*, 91: 105–120.
<https://doi.org/10.1016/j.jmst.2021.02.040>
10. Gao B, Yang Q, Zhao X, *et al.*, 2016, 4D bioprinting for biomedical applications. *Trends Biotechnol*, 34(9): 746–756.
<https://doi.org/10.1016/j.tibtech.2016.03.004>
11. Yang Q, Gao B, Xu F, 2020, Recent advances in 4D bioprinting. *Biotechnol J*, 15(1): 1900086.
<https://doi.org/10.1002/biot.201900086>
12. Kirillova A, Maxson R, Stoychev G, *et al.*, 2017, 4D biofabrication using shape-morphing hydrogels. *Adv Mater*, 29(46): 1703443.
<https://doi.org/10.1002/adma.201703443>
13. Yang GH, Yeo M, Koo YW, *et al.*, 2019, 4D bioprinting: Technological advances in biofabrication. *Macromol Biosci*, 19(5): 1800441.
<https://doi.org/10.1002/mabi.201800441>
14. Constante G, Apsite I, Alkhamis H, *et al.*, 2021, 4D biofabrication using a combination of 3D printing and melt-electrowriting of shape-morphing polymers. *ACS Appl Mater Interfaces*, 13(11): 12767–12776.
<https://doi.org/10.1021/acscami.0c18608>
15. Li J, Wu C, Chu PK, *et al.*, 2020, 3D printing of hydrogels: Rational design strategies and emerging biomedical applications. *Mater Sci Eng*, 140: 100543.
<https://doi.org/10.1016/j.mser.2020.100543>
16. Derakhshanfar S, Mbeleck R, Xu K, *et al.*, 2018, 3D bioprinting for biomedical devices and tissue engineering: A review of recent trends and advances. *Bioact Mater*, 3(2): 144–156.
<https://doi.org/10.1016/j.bioactmat.2017.11.008>
17. Lee H, Ahn S, Bonassar LJ, *et al.*, 2013, Cell-laden poly(epsilon-caprolactone)/alginate hybrid scaffolds fabricated by an aerosol cross-linking process for obtaining homogeneous cell distribution: Fabrication, seeding efficiency, and cell proliferation and distribution. *Tissue Eng Part C Methods*, 19(10), 784–793.

- <https://doi.org/10.1089/ten.tec.2012.0651>
18. Kundu J, Shim J-H, Jang J, *et al.*, 2015, An additive manufacturing-based PCL-alginate-chondrocyte bioprinted scaffold for cartilage tissue engineering. *J Tissue Eng Regen Med*, 9(11): 1286–1297.
<https://doi.org/10.1002/term.1682>
19. Kuang X, Roach DJ, Wu J, *et al.*, 2019, Advances in 4D printing: Materials and applications. *Adv Funct Mater*, 29(2): 1805290.
<https://doi.org/10.1002/adfm.201805290>
20. Bittner SM, Guo JL, Melchiorri A, *et al.*, 2018, Three-dimensional printing of multilayered tissue engineering scaffolds. *Mater Today*, 21(8): 861–874.
<https://doi.org/10.1016/j.mattod.2018.02.006>
21. Alshahrani HA, 2021, Review of 4D printing materials and reinforced composites: Behaviors, applications and challenges. *J Sci*, 6(2): 167–185.
<https://doi.org/10.1016/j.jsamd.2021.03.006>
22. Joshi S, Rawat K, Karunakaran C, *et al.*, 2020, 4D printing of materials for the future: Opportunities and challenges. *Appl Mater Today*, 18: 100490.
<https://doi.org/10.1016/j.apmt.2019.100490>
23. Wang Y, Cui H, Esworthy T, *et al.*, 2022, Emerging 4D printing strategies for next-generation tissue regeneration and medical devices. *Adv Mater*, 34(20): 2109198.
<https://doi.org/10.1002/adma.202109198>
24. Xia Y, He Y, Zhang F, *et al.*, 2021, A review of shape memory polymers and composites: Mechanisms, materials, and applications. *Adv Mater*, 33(6): 2000713.
<https://doi.org/10.1002/adma.202000713>
25. Wang L, Zhang F, Liu Y, *et al.*, 2022, Shape memory polymer fibers: Materials, structures, and applications. *Adv Fiber Mater*, 4(1): 5–23.
<https://doi.org/10.1007/s42765-021-00073-z>
26. Zhang J, Yin Z, Ren L, *et al.*, 2022, Advances in 4D printed shape memory polymers: From 3D printing, smart excitation, and response to applications. *Adv Mater Technol*, 7(9): 2101568.
<https://doi.org/10.1002/admt.202101568>
27. Khalid MY, Arif ZU, Ahmed W, 2022, 4D printing: Technological and manufacturing renaissance. *Macromol Mater Eng*, 307(8): 2200003.
<https://doi.org/10.1002/mame.202200003>
28. Alief NA, Supriadi S, Whulanza Y, 2019, Modelling the shape memory properties of 4D printed polylactic acid (PLA) for application of disk spacer in minimally invasive spinal fusion. *Proceedings of the 3rd International Symposium of Biomedical Engineering (ISBE) on Recent Progress in Biomaterials, Drugs Development, and Medical Devices: 2019*, 020005.
<https://doi.org/10.1063/1.5096673>
29. Kravtcova A, Toncheva A, Rantataro S, *et al.*, 2021, Shape memory polymer-based insertable electrode array towards minimally invasive subdural implantation. *IEEE Sens J*, 21(15): 17282–17289.
<https://doi.org/10.1109/jksen.2021.3078358>
30. Lin C, Zhang L, Liu Y, *et al.*, 2020, 4D printing of personalized shape memory polymer vascular stents with negative Poisson's ratio structure: A preliminary study. *Sci China Technol Sci*, 63(4): 578–588.
<https://doi.org/10.1007/s11431-019-1468-2>
31. Miao S, Nowicki M, Cui H, *et al.*, 2019, 4D anisotropic skeletal muscle tissue constructs fabricated by staircase effect strategy. *Biofabrication*, 11(3): 035030.
<https://doi.org/10.1088/1758-5090/ab1d07>
32. Miao S, Cui H, Nowicki M, *et al.*, 2018, Photolithographic-stereolithographic-tandem fabrication of 4D smart scaffolds for improved stem cell cardiomyogenic differentiation. *Biofabrication*, 10(3): 035007.
<https://doi.org/10.1088/1758-5090/aabe0b>
33. Miao S, Cui H, Nowicki M, *et al.*, 2018, Stereolithographic 4D bioprinting of multiresponsive architectures for neural engineering. *Adv Biosys*, 2(9): 1800101.
<https://doi.org/10.1002/adbi.201800101>
34. Miao S, Zhu W, Castro NJ, *et al.*, 2016, 4D printing smart biomedical scaffolds with novel soybean oil epoxidized acrylate. *Sci Rep*, 6: 27226.
<https://doi.org/10.1038/srep27226>
35. Zhao W, Liu L, Zhang F, *et al.*, 2019, Shape memory polymers and their composites in biomedical applications. *Mater Sci Eng C*, 97: 864–883.
<https://doi.org/10.1016/j.msec.2018.12.054>
36. Pfau MR, McKinzey KG, Roth AA, *et al.*, 2021, Shape memory polymer (SMP) scaffolds with improved self-fitting properties. *J Mater Chem B*, 9(18): 3826–3837.
<https://doi.org/10.1039/d0tb02987d>
37. Zeng X, Wang L, Chen X, *et al.*, 2022, 3D biocompatible bone engineering foams with tunable mechanical properties and porous structures. *J Appl Polym Sci*, 139(21): e52228.
<https://doi.org/10.1002/app.52228>
38. Huang X, Panahi-Sarmad M, Dong K, *et al.*, 4D printed TPU/PLA/CNT wave structural composite with intelligent thermal-induced shape memory effect and synergistically enhanced mechanical properties. *Compos Part A Appl Sci Manuf*, 158: 106946.
<https://doi.org/10.1016/j.compositesa.2022.106946>

39. Wan X, He Y, Liu Y, *et al.*, 2022, 4D printing of multiple shape memory polymer and nanocomposites with biocompatible, programmable and selectively actuated properties. *Addit Manuf*, 53: 102689.
<https://doi.org/10.1016/j.addma.2022.102689>
40. El-Husseiny HM, Mady EA, Hamabe L, *et al.*, 2022, Smart/stimuli-responsive hydrogels: Cutting-edge platforms for tissue engineering and other biomedical applications. *Mater Today Bio*, 13: 100186.
<https://doi.org/10.1016/j.mtbio.2021.100186>
41. Yesilyurt V, Webber MJ, Appel EA, *et al.*, 2016, Injectable self-healing glucose-responsive hydrogels with pH-regulated mechanical properties. *Adv Mater*, 28(1): 86–91.
<https://doi.org/10.1002/adma.201502902>
42. Shafraneck RT, Millik SC, Smith PT, *et al.*, 2019, Stimuli-responsive materials in additive manufacturing. *Prog Polym Sci*, 93: 36–67.
<https://doi.org/10.1016/j.progpolymsci.2019.03.002>
43. Willner I, 2017, Stimuli-controlled hydrogels and their applications. *Acc Chem Res*, 50(4): 657–658.
<https://doi.org/10.1021/acs.accounts.7b00142>
44. Nagase K, 2021, Thermoresponsive interfaces obtained using poly (N-isopropylacrylamide)-based copolymer for bioseparation and tissue engineering applications. *Adv Colloid Interface Sci*, 295: 102487.
<https://doi.org/10.1016/j.cis.2021.102487>
45. Tang L, Wang L, Yang X, *et al.*, 2021, Poly(N-isopropylacrylamide)-based smart hydrogels: Design, properties and applications. *Prog Mater Sci*, 115: 100702.
<https://doi.org/10.1016/j.pmatsci.2020.100702>
46. Ma Y, Hua M, Wu S, *et al.*, 2020, Bioinspired high-power-density strong contractile hydrogel by programmable elastic recoil. *Sci Adv*, 6(47): eabd2520.
<https://doi.org/10.1126/sciadv.abd2520>
47. Khoo ZX, Liu Y, An J, *et al.*, 2018, A review of selective laser melted NiTi shape memory alloy. *Materials*, 11(4): 519.
<https://doi.org/10.3390/ma11040519>
48. Sahafnejad-Mohammadi I, Karamimoghadam M, Zolfagharian A, *et al.*, 2022, 4D printing technology in medical engineering: A narrative review. *J Braz Soc Mech Sci Eng*, 44(6): 233.
<https://doi.org/10.1007/s40430-022-03514-x>
49. Yuritsa Paez-Pidiache I, Luviano-Juarez A, Lozada-Castillo N, *et al.*, 2021, Design, characterization and construction of an actuator based on shape memory alloys. *MRS Adv*, 6(39–40): 907–912.
<https://doi.org/10.1557/s43580-021-00158-2>
50. Sarraf M, Rezvani Ghomi E, Alipour S, *et al.*, 2022, A state-of-the-art review of the fabrication and characteristics of titanium and its alloys for biomedical applications. *Bio-Des Manuf*, 5(2): 371–395.
<https://doi.org/10.1007/s42242-021-00170-3>
51. Guan Z, Wang L, Bae J, 2022, Advances in 4D printing of liquid crystalline elastomers: Materials, techniques, and applications. *Mater Horiz*, 9(7): 1825–1849.
<https://doi.org/10.1039/d2mh00232a>
52. Wu J, Yao S, Zhang H, *et al.*, 2021, Liquid crystal elastomer metamaterials with giant biaxial thermal shrinkage for enhancing skin regeneration. *Adv Mater*, 33(45): 2106175.
<https://doi.org/10.1002/adma.202106175>
53. Javadzadeh M, del Barrio J, Sanchez-Somolinos C, 2023, Melt electrowriting of liquid crystal elastomer scaffolds with programmed mechanical response. *Adv Mater*, 35(14): 2209244.
<https://doi.org/10.1002/adma.202209244>
54. Lee J-H, Bae J, Hwang JH, *et al.*, 2022, Robust and reprocessable artificial muscles based on liquid crystal elastomers with dynamic thiourea bonds. *Adv Funct Mater*, 32(13): 2110360.
<https://doi.org/10.1002/adfm.202110360>
55. Hou W, Wang J, Lv J-a, 2023, Bioinspired liquid crystalline spinning enables scalable fabrication of high-performing fibrous artificial muscles. *Adv Mater*, 35(16): 2211800.
<https://doi.org/10.1002/adma.202211800>
56. Ula SW, Traugott NA, Volpe RH, *et al.*, 2018, Liquid crystal elastomers: An introduction and review of emerging technologies. *Liq Cryst Rev*, 6(1): 78–107.
<https://doi.org/10.1080/21680396.2018.1530155>
57. Lai A, Du Z, Gan CL, *et al.*, 2013, Shape memory and superelastic ceramics at small scales. *Science*, 341(6153): 1505–1508.
<https://doi.org/10.1126/science.1239745>
58. Wang F, Liu C, Yang H, *et al.*, 2023, 4D printing of ceramic structures. *Addit Manuf*, 63, 103411.
<https://doi.org/10.1016/j.addma.2023.103411>
59. Chen S, Li J, Shi H, *et al.*, 2023, Lightweight and geometrically complex ceramics derived from 4D printed shape memory precursor with reconfigurability and programmability for sensing and actuation applications. *Chem Eng J*, 455: 140655.
<https://doi.org/10.1016/j.cej.2022.140655>
60. Wang X, Zhang Y, Shen P, *et al.*, 2022, Preparation of 4D printed peripheral vascular stent and its degradation behavior under fluid shear stress after deployment. *Biomater Sci*, 10(9): 2302–2314.
<https://doi.org/10.1039/d2bm00088a>

61. Lee S, Bang D, Park J-O, *et al.*, 2022, Programmed shape-morphing material using single-layer 4D printing system. *Micromachines*, 13(2): 243.
<https://doi.org/10.3390/mi13020243>
62. Kuhnt T, Camarero-Espinosa S, Ghahfarokhi MT, *et al.*, 2022, 4D printed shape morphing biocompatible materials based on anisotropic ferromagnetic nanoparticles. *Adv Funct Mater*, 32(50): 2202539.
<https://doi.org/10.1002/adfm.202202539>
63. Siminska-Stanny J, Niziol M, Szymczyk-Ziolkowska P, *et al.*, 2022, 4D printing of patterned multimaterial magnetic hydrogel actuators. *Addit Manuf*, 49: 102506.
<https://doi.org/10.1016/j.addma.2021.102506>
64. Wang Z, Wu Y, Wu D, *et al.*, 2022, Soft magnetic composites for highly deformable actuators by four-dimensional electrohydrodynamic printing. *Compos Part B Eng*, 231: 109596.
<https://doi.org/10.1016/j.compositesb.2021.109596>
65. Dong X, Zhang F, Wang L, *et al.*, 2022, 4D printing of electroactive shape-changing composite structures and their programmable behaviors. *Compos Part A Appl Sci Manuf*, 157: 106925.
<https://doi.org/10.1016/j.compositesa.2022.106925>
66. Pineda-Castillo SA, Luo J, Lee H, *et al.*, 2021, Effects of carbon nanotube infiltration on a shape memory polymer-based device for brain aneurysm therapeutics: Design and characterization of a joule-heating triggering mechanism. *Adv Eng Mater*, 23(6): 2100322.
<https://doi.org/10.1002/adem.202100322>
67. Wang F, Wang W, Zhang C, *et al.*, 2021, Scalable manufactured bio-based polymer nanocomposite with instantaneous near-infrared light-actuated targeted shape memory and remote-controlled accurate self-healing. *Compos Part B Eng*, 219: 108927.
<https://doi.org/10.1016/j.compositesb.2021.108927>
68. Chen Y, Zhao X, Luo C, *et al.*, 2020, A facile fabrication of shape memory polymer nanocomposites with fast light-response and self-healing performance. *Compos Part A Appl Sci Manuf*, 135: 105931.
<https://doi.org/10.1016/j.compositesa.2020.105931>
69. Chen Y, Zhao X, Li Y, *et al.*, 2021, Light- and magnetic-responsive synergy controlled reconfiguration of polymer nanocomposites with shape memory assisted self-healing performance for soft robotics. *J Mater Chem C*, 9(16): 5515–5527.
<https://doi.org/10.1039/d1tc00468a>
70. Deng Y, Zhang F, Jiang M, *et al.*, 2022, Programmable 4D printing of photoactive shape memory composite structures. *ACS Appl Mater Interfaces*, 14(37): 42568–42577.
<https://doi.org/10.1021/acsami.2c13982>
71. Li M, Fu S, Lucia LA, *et al.*, 2020, Ultra-efficient photo-triggerable healing and shape-memory nanocomposite materials doped with copper sulfide nanoparticles. *Compos Sci Technol*, 199: 108371.
<https://doi.org/10.1016/j.compscitech.2020.108371>
72. Koh TY, Sutradhar A, 2022, Untethered selectively actuated microwave 4D printing through ferromagnetic PLA. *Addit Manuf*, 56: 102866.
<https://doi.org/10.1016/j.addma.2022.102866>
73. Jamal M, Kadam SS, Xiao R, *et al.*, 2013, Bio-origami hydrogel scaffolds composed of photocrosslinked PEG bilayers. *Adv Healthc Mater*, 2(8): 1142–1150.
<https://doi.org/10.1002/adhm.201200458>
74. Kwag HR, Serbo JV, Korangath P, *et al.*, 2016, A self-folding hydrogel in vitro model for ductal carcinoma. *Tissue Eng Part C Methods*, 22(4): 398–407.
<https://doi.org/10.1089/ten.tec.2015.0442>
75. Mulakkal MC, Trask RS, Ting VP, *et al.*, 2018, Responsive cellulose-hydrogel composite ink for 4D printing. *Mater Des*, 160: 108–118.
<https://doi.org/10.1016/j.matdes.2018.09.009>
76. Kim SH, Seo YB, Yeon YK, *et al.*, 2020, 4D-bioprinted silk hydrogels for tissue engineering. *Biomaterials*, 260: 120281.
<https://doi.org/10.1016/j.biomaterials.2020.120281>
77. Wu C, Chen J, Su C, 2022, 4D-printed pH sensing claw. *Anal Chim Acta*, 1204: 339733.
<https://doi.org/10.1016/j.aca.2022.339733>
78. Cao P, Yang J, Gong J, *et al.*, 2022, 4D printing of bilayer tubular structure with dual-stimuli responsive based on self-rolling behavior. *J Appl Polym Sci*, 140(1): e53241.
<https://doi.org/10.1002/app.53241>
79. Rivera-Tarazona LK, Shukla T, Singh KA, *et al.*, 2022, 4D printing of engineered living materials. *Adv Funct Mater*, 32(4): 2106843.
<https://doi.org/10.1002/adfm.202106843>
80. Grassi G, Sparrman B, Paoletti I, *et al.*, 2021, 4D soft material systems. *Proceedings of the 3rd International Conference on Computational Design and Robotic Fabrication (CDRF) (DigitalFUTURES): 2021 2021; Tongji Univ, Coll Architecture & Urban Planning, Shanghai, PEOPLES R CHINA*, 201–210.
https://doi.org/10.1007/978-981-16-5983-6_19
81. Zhou LY, Ye JH, Fu JZ, *et al.*, 2020, 4D printing of high-performance thermal-responsive liquid metal elastomers driven by embedded microliquid chambers. *ACS Appl Mater Interfaces*, 12(10): 12068–12074.
<https://doi.org/10.1021/acsami.9b22433>

82. Tang ZH, Gao ZW, Jia SH, *et al.*, 2017, Graphene-based polymer bilayers with superior light-driven properties for remote construction of 3D structures. *Adv Sci*, 4(5): 1600437.
<https://doi.org/10.1002/advs.201600437>
83. Lee AY, Zhou A, An J, *et al.*, 2020, Contactless reversible 4D-printing for 3D-to-3D shape morphing. *Virtual Phys Prototyp*, 15(4): 481–495.
<https://doi.org/10.1080/17452759.2020.1822189>
84. Deng H, Zhang C, Sattari K, *et al.*, 2021, 4D printing elastic composites for strain-tailored multistable shape morphing. *ACS Appl Mater Interfaces*, 13(11): 12719–12725.
<https://doi.org/10.1021/acsami.0c17618>
85. Qu G, Huang J, Li Z, *et al.*, 2022, 4D-printed bilayer hydrogel with adjustable bending degree for enteroatmospheric fistula closure. *Mater Today Bio*, 16: 100363.
<https://doi.org/10.1016/j.mtbio.2022.100363>
86. Hagaman DE, Leist S, Zhou J, *et al.*, 2018, Photoactivated polymeric bilayer actuators fabricated via 3D printing. *ACS Appl Mater Interfaces*, 10(32): 27308–27315.
<https://doi.org/10.1021/acsami.8b08503>
87. Liu Y, Lei Y, Hua L, *et al.*, 2021, Biomimetic self-deformation of polymer interpenetrating network with stretch-induced anisotropy. *Chem Mater*, 33(21): 8351–8359.
<https://doi.org/10.1021/acs.chemmater.1c02639>
88. Athanasopoulos N, Siakavellas NJ, 2018, Bioinspired temperature-responsive multilayer films and their performance under thermal fatigue. *Biomimetics*, 3(3): 20.
<https://doi.org/10.3390/biomimetics3030020>
89. Ding A, Jeon O, Tang R, *et al.*, 2021, Cell-laden multiple-step and reversible 4D hydrogel actuators to mimic dynamic tissue morphogenesis. *Adv Sci*, 8(9): 2004616.
<https://doi.org/10.1002/advs.202004616>
90. Ding AX, Jeon O, Cleveland D, *et al.*, 2022, Jammed microflake hydrogel for four-dimensional living cell bioprinting. *Adv Mater*, 34(15): 2109394.
<https://doi.org/10.1002/adma.202109394>
91. Ding AX, Lee SJ, Ayyagari S, *et al.*, 4D biofabrication via instantly generated graded hydrogel scaffolds. *Bioact Mater*, 7: 324–332.
<https://doi.org/10.1016/j.bioactmat.2021.05.021>
92. Ren L, Li B, He Y, *et al.*, 2020, Programming shape-morphing behavior of liquid crystal elastomers via parameter-encoded 4D printing. *ACS Appl Mater Interfaces*, 12(13): 15562–15572.
<https://doi.org/10.1021/acsami.0c00027>
93. Wu P, Yu T, Chen M, *et al.*, 2022, Effect of printing speed and part geometry on the self-deformation behaviors of 4D printed shape memory PLA using FDM. *J Manuf Process*, 84: 1507–1518.
<https://doi.org/10.1016/j.jmapro.2022.11.007>
94. Zhao W, Li N, Liu LW, *et al.*, 2022, Origami derived self-assembly stents fabricated via 4D printing. *Compos Struct*, 293: 115669.
<https://doi.org/10.1016/j.compstruct.2022.115669>
95. Tao R, Ji LT, Li Y, *et al.*, 2020, 4D printed origami metamaterials with tunable compression twist behavior and stress-strain curves. *Compos Part B Eng*, 201: 108344.
<https://doi.org/10.1016/j.compositesb.2020.108344>
96. Zhang YJ, Wang LC, Song WL, *et al.*, 2020, Hexagon-twist frequency reconfigurable antennas via multi-material printed thermo-responsive origami structures. *Front Mater*, 7: 600863.
<https://doi.org/10.3389/fmats.2020.600863>
97. Xin XZ, Liu LW, Liu YJ, *et al.*, 2020, Origami-inspired self-deployment 4D printed honeycomb sandwich structure with large shape transformation. *Smart Mater Struct*, 29(6): 065015.
<https://doi.org/10.1088/1361-665X/ab85a4>
98. Yamamura S, Iwase E, 2021, Hybrid hinge structure with elastic hinge on self-folding of 4D printing using a fused deposition modeling 3D printer. *Mater Des*, 203: 109605.
<https://doi.org/10.1016/j.matdes.2021.109605>
99. Van Manen T, Janbaz S, Jansen KMB, *et al.*, 2021, 4D printing of reconfigurable metamaterials and devices. *Commun Mater*, 2(1): 56.
<https://doi.org/10.1038/s43246-021-00165-8>
100. Ge Q, Dunn CK, Qi HJ, *et al.*, 2014, Active origami by 4D printing. *Smart Mater Struct*, 23(9): 094007.
<https://doi.org/10.1088/0964-1726/23/9/094007>
101. Yin JC, Fan WX, Xu ZH, *et al.*, 2022, Precisely defining local gradients of stimuli-responsive hydrogels for complex 2D-to-4D shape evolutions. *Small*, 18(2): 2104440.
<https://doi.org/10.1002/smll.202104440>
102. Liu G, Zhao Y, Wu G, *et al.*, 2018, Origami and 4D printing of elastomer-derived ceramic structures. *Sci Adv*, 4(8): eaat0641.
<https://doi.org/10.1126/sciadv.aat0641>
103. Langford T, Mohammed A, Essa K, *et al.*, 2021, 4D printing of origami structures for minimally invasive surgeries using functional scaffold. *Appl Sci Basel*, 11(1): 332.
<https://doi.org/10.3390/app11010332>
104. Kim D, Kim T, Lee YG, 2019, 4D printed bifurcated stents with Kirigami-inspired structures. *J Vis Exp*, 149: e59746.
<https://doi.org/10.3791/59746>

105. Ge Q, Qi HJ, Dunn ML, 2013, Active materials by four-dimension printing. *Appl Phys Lett*, 103(13): 131901.
<https://doi.org/10.1063/1.4819837>
106. Varga LG, Takacs JD, Domotor FD, *et al.*, 2018, Tailor-made 3D model design of human implants for additive technologies. *Proceedings of the 23rd International Conference on Manufacturing (Manufacturing)*.
<https://doi.org/10.1088/1757-899x/448/1/012060>
107. Lee MY, Chang CC, Lin CC, *et al.*, 2002, Custom implant design for patients with cranial defects. *IEEE Eng Med Biol Mag*, 21(2): 38–44.
<https://doi.org/10.1109/memb.2002.1000184>
108. You D, Chen G, Liu C, *et al.*, 2021, 4D printing of multi-responsive membrane for accelerated in vivo bone healing via remote regulation of stem cell fate. *Adv Funct Mater*, 31(40): 2103920.
<https://doi.org/10.1002/adfm.202103920>
109. Cui C, Kim D-O, Pack MY, *et al.*, 2020, 4D printing of self-folding and cell-encapsulating 3D microstructures as scaffolds for tissue-engineering applications. *Biofabrication*, 12(4): 045018.
<https://doi.org/10.1088/1758-5090/aba502>
110. Wang Y, Cui H, Wang Y, *et al.*, 4D printed cardiac construct with aligned myofibers and adjustable curvature for myocardial regeneration. *ACS Appl Mater Interfaces*, 13(11): 12746–12758.
<https://doi.org/10.1021/acsami.0c17610>
111. Zhang C, Cai D, Liao P, *et al.*, 2021, 4D printing of shape-memory polymeric scaffolds for adaptive biomedical implantation. *Acta Biomater*, 122: 101–110.
<https://doi.org/10.1016/j.actbio.2020.12.042>
112. Lin C, Lv J, Li Y, *et al.*, 2019, 4D-printed biodegradable and remotely controllable shape memory occlusion devices. *Adv Funct Mater*, 29(51): 1906569.
<https://doi.org/10.1002/adfm.201906569>
113. Hearon K, Wierzbicki MA, Nash LD, *et al.*, 2015, A processable shape memory polymer system for biomedical applications. *Adv Healthc Mater*, 4(9): 1386–1398.
<https://doi.org/10.1002/adhm.201500156>
114. Hu Y, Wang Z, Jin D, *et al.*, 2020, Botanical-inspired 4D printing of hydrogel at the microscale. *Adv Funct Mater*, 30(4): 1907377.
<https://doi.org/10.1002/adfm.201907377>
115. Zhou W, Duan Z, Zhao J, *et al.*, 2022, Glucose and MMP-9 dual-responsive hydrogel with temperature sensitive self-adaptive shape and controlled drug release accelerates diabetic wound healing. *Bioact Mater*, 17: 1–17.
<https://doi.org/10.1016/j.bioactmat.2024.01.004>
116. Zhang F, Wang L, Zheng Z, *et al.*, 2019, Magnetic programming of 4D printed shape memory composite structures. *Compos Part A Appl Sci Manuf*, 125: 105571.
<https://doi.org/10.1016/j.compositesa.2019.105571>
117. Zheng Y, Han MKL, Jiang Q, *et al.*, 2020, 4D hydrogel for dynamic cell culture with orthogonal, wavelength-dependent mechanical and biochemical cues. *Mater Horiz*, 7(1): 111–116.
<https://doi.org/10.1039/c9mh00665f>
118. Rosales AM, Anseth KS, 2016, The design of reversible hydrogels to capture extracellular matrix dynamics. *Nat Rev Mater*, 1(2): 15012.
<https://doi.org/10.1038/natrevmats.2015.12>
119. Farrukh A, Paez JL, del Campo A, 2019, 4D biomaterials for light-guided angiogenesis. *Adv Funct Mater*, 29(6): 1807734.
<https://doi.org/10.1002/adfm.201807734>
120. Liu L, Shadish JA, Arakawa CK, *et al.*, 2018, Cyclic stiffness modulation of cell-laden protein-polymer hydrogels in response to user-specified stimuli including light. *Adv Biosyst*, 2(12): 1800240.
<https://doi.org/10.1002/adbi.201800240>
121. Douillet C, Nicodeme M, Hermant L, *et al.*, 2022, From local to global matrix organization by fibroblasts: A 4D laser-assisted bioprinting approach. *Biofabrication*, 14(2): 025006.
<https://doi.org/10.1088/1758-5090/ac40ed>
122. Diaz-Payno PJ, Kalogeropoulou M, Muntz I, *et al.*, 2022, Swelling-dependent shape-based transformation of a human mesenchymal stromal cells-laden 4D bioprinted construct for cartilage tissue engineering. *Adv Healthc Mater*, 12(2): 2201891.
<https://doi.org/10.1002/adhm.202201891>
123. Arakawa CK, Badeau BA, Zheng Y, *et al.*, 2017, Multicellular vascularized engineered tissues through user-programmable biomaterial photodegradation. *Adv Mater*, 29(37): 1703156.
<https://doi.org/10.1002/adma.201703156>
124. Hendrikson WJ, Rouwkema J, Clementi F, *et al.*, 2017, Towards 4D printed scaffolds for tissue engineering: Exploiting 3D shape memory polymers to deliver time-controlled stimulus on cultured cells. *Biofabrication*, 9(3): 031001.
<https://doi.org/10.1088/1758-5090/aa8114>
125. Chen M, Li L, Xia L, *et al.*, 2020, Temperature responsive shape-memory scaffolds with circumferentially aligned nanofibers for guiding smooth muscle cell behavior. *Macromol Biosci*, 20(2): 1900312.
<https://doi.org/10.1002/mabi.201900312>
126. Miao S, Cui H, Esworthy T, *et al.*, 2020, 4D self-morphing culture substrate for modulating cell differentiation. *Adv Sci*, 7(6): 1902403.

- <https://doi.org/10.1002/advs.201902403>
127. Zhao Q, Wang J, Wang Y, *et al.*, 2020, A stage-specific cell-manipulation platform for inducing endothelialization on demand. *Natl Sci Rev*, 7(3): 629–643.
<https://doi.org/10.1093/nsr/nwz188>
128. Zhao W, Huang Z, Liu L, *et al.*, 2021, Porous bone tissue scaffold concept based on shape memory PLA/Fe₃O₄. *Compos Sci Technol*, 203: 108563.
<https://doi.org/10.1016/j.compscitech.2020.108563>
129. Pandey A, Singh G, Singh S, *et al.*, 2020, 3D printed biodegradable functional temperature-stimuli shape memory polymer for customized scaffoldings. *J Mech Behav Biomed Mater*, 108: 103781.
<https://doi.org/10.1016/j.jmbbm.2020.103781>
130. Wang J, Gao H, Hu Y, *et al.*, 2021, 3D printing of pickering emulsion inks to construct poly(D,L-lactide-co-trimethylene carbonate)-based porous bioactive scaffolds with shape memory effect. *J Mater Sci*, 56(1): 731–745.
<https://doi.org/10.1007/s10853-020-05318-7>
131. Hwangbo H, Lee H, Roh EJ, *et al.*, 2021, Bone tissue engineering via application of a collagen/hydroxyapatite 4D-printed biomimetic scaffold for spinal fusion. *Appl Phys Rev*, 8(2): 021403.
<https://doi.org/10.1063/5.0035601>
132. Liverani L, Liguori A, Zezza P, *et al.*, 2022, Nanocomposite electrospun fibers of poly(epsilon-caprolactone)/bioactive glass with shape memory properties. *Bioact Mater*, 11: 230–239.
<https://doi.org/10.1016/j.bioactmat.2021.09.020>
133. Kabirian F, Mela P, Heying R, 2022, 4D Printing applications in the development of smart cardiovascular implants. *Front Bioeng Biotechnol*, 10: 873453.
<https://doi.org/10.3389/fbioe.2022.873453>
134. Briggs S, Herting S, Fletcher G, *et al.*, 2022, Mechanical and shape memory properties of electrospun polyurethane with thiol-ene crosslinking. *Nanomaterials*, 12(3): 406.
<https://doi.org/10.3390/nano12030406>
135. Zhou Y, Zhou D, Cao P, *et al.*, 2021, 4D printing of shape memory vascular stent based on beta CD-g-polycaprolactone. *Macromol Rapid Commun*, 42(14): 2100176.
<https://doi.org/10.1002/marc.202100176>
136. Kuang X, Chen K, Dunn CK, *et al.*, 2018, 3D printing of highly stretchable, shape-memory, and self-healing elastomer toward novel 4D printing. *ACS Appl Mater Interfaces*, 10(8): 7381–7388.
<https://doi.org/10.1021/acsami.7b18265>
137. Lee Y, Ceylan H, Yasa IC, *et al.*, 2021, 3D-printed multi-stimuli-responsive mobile micromachines. *ACS Appl Mater Interfaces*, 13(11): 12759–12766.
<https://doi.org/10.1021/acsami.0c18221>
138. Feng J, Shi H, Yang X, *et al.*, 2021, Self-adhesion conductive sub-micron fiber cardiac patch from shape memory polymers to promote electrical signal transduction function. *ACS Appl Mater Interfaces*, 13(17): 19593–19602.
<https://doi.org/10.1021/acsami.0c22844>
139. Lin C, Liu L, Liu Y, *et al.*, 2021, 4D printing of bioinspired absorbable left atrial appendage occluders: A proof-of-concept study. *ACS Appl Mater Interfaces*, 13(11): 12668–12678.
<https://doi.org/10.1021/acsami.0c17192>
140. Lin C, Huang Z, Wang Q, *et al.*, 2022, 4D printing of overall radiopaque customized bionic occlusion devices. *Adv Healthc Mater*, 12(4): 2201999.
<https://doi.org/10.1002/adhm.202201999>
141. Haykal S, Salna M, Waddell TK, *et al.*, 2014, Advances in tracheal reconstruction. *Plast Reconstruct Surg Glob Open*, 2(7): e178.
<https://doi.org/10.1097/gox.0000000000000097>
142. Murgu SD, Colt HG, 2006, Tracheobronchomalacia and excessive dynamic airway collapse. *Respirology*, 11(4): 388–406.
<https://doi.org/10.1111/j.1440-1843.2006.00862.x>
143. Freitag L, Goerdes M, Zarogoulidis P, *et al.*, 2017, Towards individualized tracheobronchial stents: Technical, practical and legal considerations. *Respiration*, 94(5): 442–456.
<https://doi.org/10.1159/000479164>
144. Maity N, Mansour N, Chakraborty P, *et al.*, 2021, A personalized multifunctional 3D printed shape memory-displaying, drug releasing tracheal stent. *Adv Funct Mater*, 31(50): 2108436.
<https://doi.org/10.1002/adfm.202108436>
145. Zarek M, Mansour N, Shapira S, *et al.*, 2017, 4D printing of shape memory-based personalized endoluminal medical devices. *Macromol Rapid Commun*, 38(2): 1600628.
<https://doi.org/10.1002/marc.201600628>
146. Zhang F, Wen N, Wang L, *et al.*, 2021, Design of 4D printed shape-changing tracheal stent and remote controlling actuation. *Int J Smart Nano Mater*, 12(4): 375–389.
<https://doi.org/10.1080/19475411.2021.1974972>
147. Zhao W, Zhang F, Leng J, *et al.*, 2019, Personalized 4D printing of bioinspired tracheal scaffold concept based on magnetic stimulated shape memory composites. *Compos Sci Technol*, 184: 107866.
<https://doi.org/10.1016/j.compscitech.2019.107866>
148. Pandey H, Mohol SS, Kandi R, 2022, 4D printing of tracheal scaffold using shape-memory polymer composite. *Mater Lett*, 329: 133238.
<https://doi.org/10.18063/ijb.764>

- <https://doi.org/10.1016/j.matlet.2022.133238>
149. Yang GH, Kim W, Kim J, *et al.*, 2021, A skeleton muscle model using GelMA-based cell-aligned bioink processed with an electric-field assisted 3D/4D bioprinting. *Theranostics*, 11(1): 48–63.
<https://doi.org/10.7150/thno.50794>
150. Cui H, Miao S, Esworthy T, *et al.*, 2019, A novel near-infrared light responsive 4D printed nanoarchitecture with dynamically and remotely controllable transformation. *Nano Res*, 12(6): 1381–1388.
<https://doi.org/10.1007/s12274-019-2340-9>
151. Esworthy TJ, Miao S, Lee S-J, *et al.*, 2019, Advanced 4D-bioprinting technologies for brain tissue modeling and study. *Int J Smart Nano Mater*, 10(3): 177–204.
<https://doi.org/10.1080/19475411.2019.1631899>
152. Fang J-H, Hsu H-H, Hsu R-S, *et al.*, 2020, 4D printing of stretchable nanocookie@conduit material hosting biocues and magnetoelectric stimulation for neurite sprouting. *NPG Asia Mater*, 12(1): 61.
<https://doi.org/10.1038/s41427-020-00244-1>
153. Deng Y, Yang B, Zhang F, *et al.*, 2022, 4D printed orbital stent for the treatment of enophthalmic invagination. *Biomaterials*, 291: 121886.
<https://doi.org/10.1016/j.biomaterials.2022.121886>
154. Miao S, Castro N, Nowicki M, *et al.*, 2017, 4D printing of polymeric materials for tissue and organ regeneration. *Mater Today*, 20(10): 577–591.
<https://doi.org/10.1016/j.mattod.2017.06.005>
155. Zu S, Wang Z, Zhang S, *et al.*, 2022, A bioinspired 4D printed hydrogel capsule for smart controlled drug release. *Mater Today Chem*, 24: 100789.
<https://doi.org/10.1016/j.mtchem.2022.100789>
156. Zu S, Zhang Z, Liu Q, *et al.*, 2022, 4D printing of core-shell hydrogel capsules for smart controlled drug release. *Bio-Des Manuf*, 5(2): 294–304.
<https://doi.org/10.1007/s42242-021-00175-y>
157. Zhang Y, Yang G, Hayat U, *et al.*, 2023, Water-responsive 4D printing based on self-assembly of hydrophobic protein “Zein” for the control of degradation rate and drug release. *Bioact Mater*, 23: 343–352.
<https://doi.org/10.1016/j.bioactmat.2022.11.009>